1

Linear Optimal Control for Autonomous Pattern Generation

Taylor Ludeke and Tetsuya Iwasaki

Abstract-An important objective in the design of feedback control systems is the pattern generation. The term 'pattern' denotes the behavior of the individual plant states relative to one another in steady-state, e.g. periodic with a specified frequency and phase offset. Here we solve the optimal, linear, output feedback problem in which the controller is autonomous, achieves pattern generation, and minimizes the L_2 norm of the transient portion of the impulse response. Our result reveals the optimal control architecture comprising a linear quadratic regulator and a Kalman filter, along with additional feedback/feedforward to/from a pattern generator, with gains constrained by the regulator equation and its dual, respectively. In contrast to the standard output regulation, the pattern generator is embedded in the feedback loop, allowing the reference signals to be modified autonomously in response to disturbances. A design example illustrates the controller's ability to recalculate and track the target trajectory following a disturbance.

Index Terms—Optimal control, eigenstructure assignment, pattern formation, autonomous control, linear systems

I. INTRODUCTION

Pattern formation is a process of dynamical systems in which the state converges to a persistent trajectory with a specific spatiotemporal property in the steady state. Various phenomena in nature exhibit such behaviors [1]: blinking fireflies, bird flocking, fish schooling, hurricanes, neural oscillator network, and periodic gaits in animal locomotion. Partly motivated by such natural phenomena, pattern formation is also central to certain engineering designs, including bio-inspired mobile robots, aircraft/satellite formations, vehicle platooning, and swarm robotics. The associated technical problems are often formulated in some abstracted form, such as multiagent coordination and coupled oscillator synchronization [2]–[4]. The theory of pattern formation would have a broad range of applications extending to economic and social studies.

A standard way to achieve persistent steady-state trajectories is by output regulation which tracks a persistent signal generated by an exosystem with an internal model in the controller [5]–[8]. This method is advantageous when the reference trajectory is fixed regardless of the operating condition. Alternatively, embedding the pattern generator in the feedback loop such that the closed-loop system is autonomous, allows the controller to adjust the reference signal in response to disturbances and changes in the environment.

Autonomous control architecture is found in biology. The central pattern generator (CPG) is a neuronal circuit that commands rhythmic muscle contractions during animal locomo-

The authors are with the Department of Mechanical and Aerospace Engineering, University of California, Los Angeles, 420 Westwood Plaza, Los Angeles, CA 90095, {tludeke,tiwasaki}@ucla.edu.

tion [9]–[11]. The CPG creates a basic gait when isolated, and has the ability to adjust the gait autonomously in accordance with the sensory feedback information [12]. Such capability for autonomous oscillations is valuable in the design of robotic locomotion systems where various gait patterns are generated as stable limit cycles [13]–[15]. Also in some context of engineering, feedback mechanisms for multiagent coordination or coupled oscillator synchronization are typically designed to make a global pattern emerge autonomously from the network formed by local interactions, rather than from forced response driven by an exosystem.

In the control of multiple subsystems, consensus or synchronization can readily be achieved autonomously if the subsystems are homogeneous and share the same target dynamics [16]–[20]. The idea is to stabilize the synchronous subspace by diffusive network connections that functionally vanish in the subspace. For heterogeneous subsystems, a clean solution is available within the framework of the output regulation if autonomy is not required and each subsystem can be forced to track a command from a network of homogeneous reference generators [21]. However, the problem is much harder when autonomy is required, and early results relied on special properties (e.g. minimum phase, small gain) to guarantee synchronization [22]-[24]. More recently, the framework of eigenstructure assignment has provided a new perspective on autonomous control for constant formation [25], modal consensus [26], and general coordination [27] of heterogeneous subsystems with endogenous or explicit internal models.

Eigenstructure assignment is a classical subject in control theory where the goal is to assign a given set of eigenvalues and eigenvectors to the closed-loop system using a feedback controller [28], [29]. Methods have been developed to tackle various control problems over the years including decoupling of flight modes for improved control [30], [31] and vibration suppression [32]. The classical theory of eigenstructure assignment was limited by the small design freedom associated with static state/output feedback. However, an expansion of the design space to include dynamic feedback has allowed for an exact characterization of assignable eigenstructures in terms of the regulator equation, and a parametrization of all controllers that assign a given eigenstructure [27]. More importantly, the result provided a bridge between traditional output regulation and autonomous pattern formation, and a general framework for heterogeneous multiagent coordination.

In this paper, we consider the optimal eigenstructure assignment problem for linear systems. A special case of this where the target dynamics of the exosystem are augmented within the generalized plant, i.e., the optimal output regulation

problem, has been solved with some generality in the literature [33]. When autonomous pattern formation is considered for a general class of plants, however, the problem remains open (or has not even been posed) and no solution has been available even when the controller is centralized to allow for an arbitrary (all-to-all) network topology. We solve the problem under the stabilizability assumption (which excludes the output regulation problem) for the centralized case, which is directly relevant for pattern formation in mechanical systems with multiple degrees of freedom, such as gait generation in robotic locomotion systems. Moreover, our result would lay a theoretical foundation for optimal multiagent coordination.

We solve an optimal control problem for linear output feedback that meets the following criteria: 1) The controller achieves pattern generation for the closed-loop system with an arbitrary initial state, for which the target behavior is described by persistent signals in the steady-state; periodic, constant, growing, or a combination. 2) The controller minimizes an H_2 cost function, or the L_2 norm of the transient portion of the impulse response. The pattern is prescribed by an eigenstructure (a set of eigenvalues and eigenvectors), but the actual trajectory, to which the state converges, depends on the initial state and/or disturbances that affect the magnitude and time shift. The optimal controller turns out to be autonomous such that a pattern generator is embedded within the feedback loop, allowing for the controller to respond to (impulse) disturbances by optimizing the freedom in the target trajectory to minimize the transient cost.

Our approach is to exploit a parametrization of all controllers assigning a given eigenstructure [27], and perform an analytical optimization in the state space. The control architecture is given by diffusive coupling of the plant and a pattern generator, with the design freedom in the coupling dynamics. The main challenge is the lack of an explicit characterization of the transient cost due to the fact that, by design, the closed-loop system is not stabilized, invalidating the standard characterizations of the H_2 norm using Gramians. The key idea is to find a state transformation that allows for decomposition of the closed-loop system into the steady-state dynamics for the target pattern and the transient dynamics that define the cost for optimization. We find that the dual of the regulator equation plays a major role for the decomposition.

Once decomposed, the problem reduces to a standard H_2 control problem except for the dependence of the generalized plant on additional design parameters — the solution of the dual regulator equation, which substantially complicates the design. We develop an extension of the change of variables used for multiobjective control [34], [35] and convert the problem to a convex optimization in terms of linear matrix inequalities (LMIs). While the optimal controller can be computed by the LMI optimization, we proceed further to gain analytical insights and reveal the optimal control architecture. As a result, the design reduces to the standard two Riccati equations for the optimal H_2 control, and an additional convex optimization over solutions of the dual regulator equation.

The optimal control architecture is found analogous to the Youla parametrization [36], and is described by the standard Kalman filter and the linear quadratic regulator (LQR), plus a

pattern generator. The solution of the dual regulator equation defines the feedback gain to the pattern generator which determines the optimal target trajectory based on the feedback information. The solution of the regulator equation defines the feedforward gain from the pattern generator to add input to the standard H_2 control to achieve the steady state pattern. The result reveals the profound symmetry/duality of the optimal control architecture. While the Kalman gain and the LQR gain are computed independently of the solutions to the primal/dual regulator equations, the separation principle does not hold in the sense that the optimal output feedback control cannot be recovered by adding the Kalman filter to the optimal state feedback because the optimal feedback gain to the pattern generator for the output feedback is different from the one for the state feedback in general.

The main contributions of this paper can be summarized as follows. We add a fundamental result to the body of literature on linear optimal control theories by formulating and solving a novel problem of optimal autonomous pattern generation within the framework of eigenstructure assignment. The optimal control is shown to have the architecture of the Youla parametrization, where the LQR and Kalman filter are interfaced with a pattern generator through solutions to the primal/dual regulator equations in a linear fractional manner. The new theory complements and extends the traditional output regulation theory toward autonomous motion coordination, and lays a foundation for various applications such as consensus/synchronization of multiple agents and gait generation for robotic locomotion systems.

A preliminary result has been reported in [37], where we solved the optimal eigenstructure assignment for the state feedback case to minimize a quadratic cost on the initial state response. The class of controllers for optimization was limited to those with the pattern generator plus static state feedback. Here we provide a result for the general dynamic output feedback to optimize the H_2 performance with respect to arbitrarily specified input-output channels.

We use the following notation. For a square matrix A, $\operatorname{eig}(A)$ denotes the set of eigenvalues of A, and $\operatorname{He}(A)$ is the Hermitian part $\operatorname{He}(A) := A + A^{\mathsf{T}}$. Notations $\operatorname{diag}(M_1,\ldots,M_n)$, $\operatorname{col}(M_1,\ldots,M_n)$, and $\operatorname{row}(M_1,\ldots,M_n)$ denote the matrices obtained by stacking matrices M_i with $i=1,\ldots,n$ on the diagonal, column, and row, respectively. For real symmetric matrices A and B, inequality A>B means that A-B is positive definite. For a transfer function $\mathfrak{F}_s(s)$, its H_2 norm is denoted by $\|\mathfrak{F}_s\|_2$. A state space system with realization Θ is denoted by \mathfrak{G} , that is, the system

$$\left[\begin{array}{c} \dot{x} \\ y \end{array}\right] = \Theta \left[\begin{array}{c} x \\ u \end{array}\right], \quad \Theta := \left[\begin{array}{cc} A & B \\ C & D \end{array}\right]$$

is expressed as

$$y = \mathring{\Theta}u, \quad \mathring{\Theta} = \left(\begin{array}{c|c} A & B \\ \hline C & D \end{array}\right),$$

where x, u, and y are the state, input, and output. Note that $\mathring{\Theta}$ is a system (an operator that maps a signal to a signal), while Θ is a constant matrix that defines the system $\mathring{\Theta}$. Lastly, $\alpha(t) \to \beta(t)$ means $\|\alpha(t) - \beta(t)\|$ approaches zero as $t \to \infty$.

II. PROBLEM FORMULATION

A. Problem Statement

Consider the generalized plant described by

$$\dot{x} = Ax + B_1 w + B_2 u,
p = C_p x + D_p u,
z = C_1 x + D_1 u,
y = C_2 x + D_2 w,$$
(1)

where $x(t) \in \mathbb{R}^n$ is the state, $u(t) \in \mathbb{R}^{n_u}$ is the control input, $y(t) \in \mathbb{R}^{n_y}$ is the measured output available for feedback control, $w(t) \in \mathbb{R}^{n_w}$ is the disturbance input, and $z(t) \in \mathbb{R}^{n_z}$ and $p(t) \in \mathbb{R}^{n_p}$ are the performance outputs. The objective is to determine an optimal controller $u = \mathring{K}y$ that achieves pattern formation for output p(t) in the steady state while minimizing a transient cost associated with z(t).

The pattern formation constraint in the control design is described by the convergence property

$$p(t) \to \Pi e^{\Lambda t} \rho_o$$
 (2)

for the closed-loop system with an arbitrary initial state under no disturbance input (w(t)=0), where the matrix pair $(\Pi,\Lambda)\in\mathbb{R}^{n_p\times r}\times\mathbb{R}^{r\times r}$ prescribes the target pattern and ρ_o is an arbitrary vector that depends on the initial state. Since (2) specifies the steady state behavior, the pattern should contain no decaying term. Thus we impose the following.

Assumption 1: Λ has no eigenvalue with negative real part. For practical purposes, Λ would typically have eigenvalues on the imaginary axis to achieve convergence to oscillations or constants. When Λ has an eigenvalue with positive real part, the response would diverge and the design may not be useful. However, we do not exclude this case to keep generality of the theory developed in this paper. Also, such case may become useful for achieving convergence to prescribed constants by introducing saturation nonlinearities, which is beyond the scope of this paper but may be addressed in the future.

The convergence property (2) is ensured by an appropriate eigenstructure for the closed-loop system, defined as follows.

Definition 1: Consider the plant (1), target pattern (Π, Λ) , and controller $u = \mathring{K}y$ with state vector x_{κ} . Let the unforced $(w(t) \equiv 0)$ dynamics of the closed-loop system be described by $\dot{\mathbf{x}} = \mathbf{A}_{c\ell}\mathbf{x}$ and $p = \mathbf{H}_{c\ell}\mathbf{x}$ with $\mathbf{x} = col(x, x_{\kappa})$. The controller is said to be admissible if the following conditions

$$\mathbf{A}_{c\ell} \mathbf{X}_{c\ell} = \mathbf{X}_{c\ell} \Lambda, \quad \Pi = \mathbf{H}_{c\ell} \mathbf{X}_{c\ell}, \\ eig(\mathbf{A}_{c\ell}) \backslash eig(\Lambda) \in \mathbb{C}_{-}$$
 (3)

hold for some full column rank $X_{c\ell}$, where \mathbb{C}_- is the set of complex numbers with negative real parts. The set of admissible controllers is denoted by \mathbb{A} .

Condition (3) specifies that the closed-loop system has the eigenstructure $(X_{c\ell}, \Lambda)$ and all the eigenvalues of $\mathbf{A}_{c\ell}$ except for those shared with Λ are in the open left half plane. By the standard linear system theory, every state trajectory converges to the range space of $X_{c\ell}$, in which the temporal dynamics is specified by Λ . Thus (3) implies $\mathbf{x}(t) \to \mathbf{X}_{c\ell} e^{\Lambda t} \rho_o$ for some vector ρ_o , and $\Pi = \mathbf{H}_{c\ell} \mathbf{X}_{c\ell}$ then ensures (2). Conversely, necessity of (3) for pattern generation (2) can be formally proven through the concept of asymptotic equivalence [27].

Let us now define the cost function to be minimized over the set of admissible controllers $\mathring{\mathcal{K}} \in \mathbb{A}$. The closed-loop transfer function from w to z, denoted by $\mathfrak{F}(s)$, has the dynamics dictated by the eigenvalues of $\mathbf{A}_{c\ell}$. When the controller is admissible, $\mathbf{A}_{c\ell}$ is similar to $\mathrm{diag}(\Lambda, \mathbf{A})$ for some Hurwitz matrix \mathbf{A} due to (3), and $\mathfrak{F}(s)$ can be decomposed as

$$\mathfrak{F}(s) = \mathfrak{F}_a(s) + \mathfrak{F}_s(s),\tag{4}$$

where $\mathfrak{F}_a(s)$ is anti-stable with eigenvalues of Λ , and $\mathfrak{F}_s(s)$ is stable with eigenvalues of \mathbf{A} . The cost function we seek to minimize is the square of the H_2 norm of the stable part:

$$\gamma(\mathring{\mathcal{K}}) := \|\mathfrak{F}_s\|_2^2. \tag{5}$$

The basic problem we address is formally stated as follows. Problem 1: Consider the plant (1) and the set of admissible controllers \mathbb{A} as described in Definition 1 for a given target

controllers $\mathbb A$ as described in Definition 1 for a given target pattern (Π, Λ) satisfying Assumption 1. Solve

$$\gamma_* := \inf_{\mathring{\kappa} \in \mathbb{A}} \gamma(\mathring{K}), \tag{6}$$

i.e., determine an admissible controller $\check{K} \in \mathbb{A}$ that gives the cost value $\gamma(\check{K})$ equal (or arbitrarily close) to γ_* .

The cost function (5) defined in the frequency domain has a time domain interpretation based on the Plancherel's equality [38], i.e., the H_2 norm of a scalar transfer function is equal to the L_2 norm of its impulse response. Suppose the initial state of the closed-loop system is zero, $\mathbf{x}(0)=0$. When an impulsive disturbance $w(t)=w_o\delta(t)$ is applied to the closed-loop system, we have, from the decomposition (4),

$$z(t) \to z_a(t) := Ze^{\Lambda t}\rho_o, \quad \rho_o := Ww_o,$$
 (7)

where $\delta(t)$ is the Dirac delta function, and Z and W are the state space matrices of $\mathfrak{F}_a(s)$:

$$\mathfrak{F}_a(s) = Z(sI - \Lambda)^{-1}W.$$

For fast convergence, we penalize the transient $z_s:=z-z_a$, which is the impulse response of the stable part $\mathfrak{F}_s(s)$. Let z^k be the response to the impulse with $w_o=e_k$, and z_s^k be the corresponding transient output, where e_k is the $k^{\rm th}$ column of the $n_w\times n_w$ identity matrix. By Plancherel's equality, the cost function γ is then given in terms of the L_2 norm of $z_s^k(t)$, summed over all directions of $w_o\in\mathbb{R}^{n_w}$ as follows:

$$\gamma(\mathring{\kappa}) = \sum_{k=1}^{n_w} \int_0^\infty \|z_s^k(t)\|^2 dt.$$
 (8)

Thus, the problem is to design an optimal controller $\mathring{\mathcal{K}}$ that achieves convergence of p(t) as in (2) with an arbitrary initial state, while minimizing the transient cost $\gamma(\mathring{\mathcal{K}})$ associated with z(t) in response to the impulse disturbance in w(t).

B. Significance

The optimal eigenstructure assignment formulated as Problem 1 has various applications to which traditional control theories do not apply. The main distinction is that the closed-loop system is not stabilized by the design, but rather is forced to embed unstable dynamics Λ . One of the simplest examples that motivate our problem is bringing a sliding block to an

arbitrary, stationary position after the block has experienced an impulsive disturbance force. The problem is to design a controller $u=\mathring{\kappa}y$ such that $\dot{y}(t)\to 0$ for the plant

$$\ddot{y} = u + w$$
, $w(t) = \delta(t)$.

Since y(t) is allowed to converge to a nonzero constant, the closed-loop system should not be stabilized, but should have an eigenvalue $\Lambda=0$.

This type of design requirements can be generalized as the pattern generation for vector variable p as in (2), where $\Lambda \in \mathbb{R}^{r \times r}$ determines the temporal pattern (oscillation, constant, growth) and $\Pi \in \mathbb{R}^{n_p \times r}$ the spatial pattern (relative amplitudes/phases) as described in [27]. For example, an oscillation pattern $o_i(t) = a_i \sin(\omega t + b_i)$ is specified by

$$\Lambda = \begin{bmatrix} 0 & \omega \\ -\omega & 0 \end{bmatrix}, \qquad \begin{aligned} \Pi &= \operatorname{col}(\Pi_1, \dots, \Pi_{n_p}), \\ \Pi_i &:= \begin{bmatrix} a_i \cos(b_i) & a_i \sin(b_i) \end{bmatrix}, \end{aligned}$$

and (2) is equivalent to $p_i(t) \to \alpha o_i(t+\tau)$ where (α,τ) is specified by $\rho_o \in \mathbb{R}^2$. It should be noted that the design requirement in (2) specifies the oscillation pattern by (Π,Λ) but its spatial size α and temporal phase τ are not prescribed by the design constraint since ρ_o is arbitrary. This property holds for the general case of (2), i.e., the pattern is specified by (Π,Λ) but the size and phase are left unspecified within the freedom of ρ_o . Thus, Problem 1 is distinct from the traditional optimal tracking problem with a completely prescribed target trajectory, and aims at the control design for the optimal autonomous behavior with the ability to adjust the target trajectory when perturbed by disturbances.

During a steady operation of the control system, disturbances can perturb the state away from the desired trajectory. The controller is tasked to make the state converge back to a steady operation, which may not have to be the same trajectory as the one before the disturbance. For example, the temporal phase of an oscillatory trajectory does not matter for steady progress of robotic locomotion systems. Hence, the target trajectory should be adjusted in real time to achieve fast and efficient return to the steady operation. Our design captures this desired property by the freedom ρ_o in (2). Formalizing the perturbation by the impulse disturbance $w(t) = w_o \delta(t)$, where w_o specifies the direction and magnitude of the perturbation, we recognize that ρ_o is a function of w_o ; in fact, $\rho_o = W w_o$ as in (7). The controller that solves Problem 1 specifies W so that the optimal steady state trajectory for the given perturbation w_o is selected to minimize the transient.

We focus on minimization of the H_2 norm, which is equivalent to the L_2 norm of the impulse response as shown earlier. This time-domain interpretation is directly related to the cost in the classical linear quadratic regulator (LQR). The H_2 performance can also be interpreted in terms of the output variance in response to stochastic noises as is well known in the linear quadratic Gaussian (LQG) control. Yet another interpretation of the H_2 norm is the energy-to-peak gain, which is the largest L_∞ norm of the output among those resulting from all possible disturbances with L_2 norm less than or equal to one [39]. Thus, the cost function (5) has multiple interpretations relevant for various applications. Moreover, as we point out in Section IV-A, the theory we develop for the

 H_2 performance can be applied, with slight modifications, to multiobjective control with various performance measures, including the energy-to-energy gain (i.e. H_{∞} norm) and upper bounds on the impulse-to-peak and peak-to-peak gains [34].

Based on the internal model principle [27], the design specification (2) requires that the target dynamics Λ be embedded in the feedback controller as a pattern generator. In general, the pattern generator receives sensory signals from the plant, which allows for real-time adjustment of the size and timing of the pattern in response to disturbances and changes in the environment. This is distinct from the standard paradigm of the output regulation [5], [7], [8], where an exogenous system sits outside of the feedback loop and generates a fixed command pattern, and a feedback controller is designed to achieve exact tracking. The autonomous pattern generation with sensory feedback is found in biological control mechanisms that exhibit adaptive behaviors [12], and is advantageous for certain engineering applications such as robotic locomotion [15] and multiagent coordination [20], [40].

C. Preliminaries from Eigenstructure Assignment Theory

This section provides a basis for solving Problem 1 by reviewing and extending some results from [27], which essentially solved the feasibility part of the problem. In particular, [27] characterized when the set \mathbb{A} of admissible controllers is nonempty, and gave a parametrization of an essential subset of \mathbb{A} . The following lemma shows that any cost (5) achieved by an admissible controller can be achieved by a controller in this subset. The implication is that the optimization over the subset is equivalent to the original problem in (6).

Lemma 1: Consider the plant (1) and target dynamics (Π, Λ) , where Assumption 1 holds and (C_2, A) is detectable. The set of admissible controllers \mathbb{A} in Definition 1 is nonempty if and only if there exists a matrix pair (X, U) such that

$$X\Lambda = AX + B_2U,$$

$$\Pi = C_nX + D_nU,$$
(9)

hold and $(A, B_2^{\mathbf{x}})$ is stabilizable, where $B_2^{\mathbf{x}} := [B_2 - X]$. Consider Problem 1 and the infimum cost value γ_* . Let γ_o be an arbitrary feasible cost, i.e., $\gamma_o > \gamma_*$. Then a controller $\mathring{K} \in \mathbb{A}$ such that $\gamma(\mathring{K}) = \gamma_o$ is given by

$$\begin{bmatrix} u \\ \dot{\xi} \end{bmatrix} = \begin{bmatrix} U \\ \Lambda \end{bmatrix} \xi + \mathring{\Theta}(y - C_2 X \xi)$$
 (10)

for some $\overset{\circ}{\Theta}$ that stabilizes the augmented plant $(A, B_2^{\mathbf{x}}, C_2)$ and for some (X, U) satisfying (9). For this controller, the unforced $(w(t) \equiv 0)$ closed-loop trajectory satisfies

$$\begin{array}{ll} x(t) \rightarrow X \xi_o(t), & p(t) \rightarrow \Pi \xi_o(t), & \xi(t) \rightarrow \xi_o(t), \\ u(t) \rightarrow U \xi_o(t), & z(t) \rightarrow Z \xi_o(t), & \xi_o(t) := e^{\Lambda t} \rho_o, \end{array} \tag{11}$$

for some $\rho_o \in \mathbb{R}^r$ depending on the initial state, where

$$Z := C_1 X + D_1 U. \tag{12}$$

Proof. See Appendix A.

The controller formula (10) parametrizes a subset of \mathbb{A} in terms of (X, U) satisfying (9) and $\overset{\circ}{\Theta}$ stabilizing $(A, B_2^{\mathbf{x}}, C_2)$. Lemma 1 shows that an arbitrary feasible cost γ_o can be

achieved by a controller of the form (10). Hence an optimal (or near optimal) controller solving (6) belongs to this subset, and Problem 1 can be solved by minimizing $\gamma(\mathring{\kappa})$ over (X,U) and $\mathring{\Theta}$. Thus, the explicit parametrization of controllers as in (10) is directly useful for solving Problem 1.

The parameter pair (X,U) satisfying (9) is not unique in general and the choice will affect the transient cost. However, we will focus on the optimization after the choice is made. Since (X,U) specifies the steady state behavior as in (11), it may be chosen to optimize the cost for maintenance of the target pattern $p(t) = \Pi e^{\Lambda t} \rho_o$. For instance, the magnitude of the control input $\|U\|$ may be minimized over (X,U) satisfying (9), which can readily be solved using a semidefinite programming package since the norm $\|U\|$ is a convex function of U and constraint (9) is linear in (X,U). Once (X,U) is fixed, the cost (5) can be optimized over Θ . To make a formal statement of this problem, let us introduce:

Assumption 2:

- (i) For the target pattern (Π, Λ) , a pair (X, U) exists and is fixed such that (A, B_2^x) is stabilizable and (9) holds.
- (ii) (C_2, A) is detectable.

For a given pair (X, U), let $\mathbb{A}_o \subset \mathbb{A}$ be the subset of admissible controllers captured by (10) with some $\overset{\circ}{\Theta}$ stabilizing $(A, B_2^{\mathbf{x}}, C_2)$. The problem is then formulated as follows.

Problem 2: Consider Problem 1 and suppose Assumption 2 holds. Solve Problem 1 with \mathbb{A} replaced with \mathbb{A}_0 .

The rest of the paper is focused on solving Problem 2, which is not equivalent to Problem 1 since (X,U), i.e., the relative spatial sizes and temporal phases of (x,u), is fixed. The optimal cost value of Problem 1 is always no worse than that of Problem 2 since (X,U) is chosen to optimize the transient cost in Problem 1. However, Problem 2 may be more practically valuable than Problem 1 since it would make more sense to also penalize the steady state cost during the design, justifying a separate optimization of (X,U) as described above.

III. REFORMULATION VIA DUAL REGULATOR EQUATION

A. Overview of the Approach

Problem 2 is much more difficult than traditional optimal control problems, which focus on stabilization of the closed-loop system, due to the fact that the autonomous pattern formation requires the closed-loop system to have eigenvalues with nonnegative real parts to achieve convergence, not to the origin, but to a pattern. Also by the requirement of autonomy, the target steady state trajectory is not prescribed, which makes the dependence of the transient cost on the controller much more complex than in the traditional optimal control theories.

We will solve Problem 2 through a series of reparametrizations of the feasible controller set \mathbb{A}_o as follows:

$$\mathbb{A}_o \leftrightarrow \mathbb{A}_1 \leftrightarrow \mathbb{A}_2, \quad \bar{\mathbb{A}}_2 = \bar{\mathbb{A}}_3, \quad \mathbb{A}_3 \leftrightarrow \mathbb{A}_4 \leftrightarrow \mathbb{A}_5, \quad (13)$$

where $\mathbb{A}_i \leftrightarrow \mathbb{A}_j$ indicates existence of a bijective mapping between the two sets \mathbb{A}_i and \mathbb{A}_j , and $\bar{\mathbb{A}}_i$ denotes the closure of \mathbb{A}_i . Problem 2 is reduced to a constrained H_2 optimization over \mathbb{A}_2 using a Sylvester equation, and then eventually to an unconstrained H_2 optimal control problem over \mathbb{A}_5 using a

dual regulator equation. This section provides an overview of this approach, while the sections that follow will provide the details and theoretical justifications.

To explain the idea, let us introduce some system matrices. Let the state space realization of Θ in (10) be denoted by

$$\mathring{\Theta} = \begin{pmatrix} A_{\theta} & B_{\theta} \\ \hline C_{\theta} & D_{\theta} \end{pmatrix}, C_{\theta} = \begin{bmatrix} C_{\theta 1} \\ C_{\theta 2} \end{bmatrix}, D_{\theta} = \begin{bmatrix} D_{\theta 1} \\ D_{\theta 2} \end{bmatrix}, (14)$$

where each of C_{θ} and D_{θ} is partitioned in accordance with the row dimensions of U and Λ , and define

$$\mathring{\Psi} = \left(\begin{array}{c|c} A_{\theta} & B_{\theta} \\ \hline C_{\theta 1} & D_{\theta 1} \end{array}\right), \quad \Gamma := \begin{bmatrix} C_{\theta 2} & D_{\theta 2} \end{bmatrix}, \quad (15)$$

so that $\Theta = \operatorname{col}(\Psi, \Gamma)$. We also define augmented matrices

$$\begin{bmatrix} \hat{A} & \hat{B}_1 & \hat{B}_2 \\ \hat{C}_1 & 0 & \hat{D}_1 \\ \hat{C}_2 & \hat{D}_2 & 0 \end{bmatrix} := \begin{bmatrix} A & 0 & B_1 & 0 & B_2 \\ 0 & 0 & 0 & I & 0 \\ \hline C_1 & 0 & 0 & 0 & D_1 \\ \hline 0 & I & 0 & 0 & 0 \\ C_2 & 0 & D_2 & 0 & 0 \end{bmatrix},$$

$$\hat{X} := \begin{bmatrix} X \\ 0 \end{bmatrix}, \quad \hat{U} := \begin{bmatrix} 0 \\ U \end{bmatrix}, \quad \begin{array}{ccc} \hat{B}_2^{\mathbf{x}} := \begin{bmatrix} & \hat{B}_2 & -\hat{X} \\ & \hat{D}_1^{\mathbf{x}} := \begin{bmatrix} & \hat{D}_1 & 0 \end{bmatrix}, \end{array}$$

where the sizes of the zero and identity matrices should become clear from the context.

By definition, A_o is parametrized by (10) with Θ in

$$\mathbb{A}_1 := \{ \Theta : \ \hat{A} + \hat{B}_2^{\mathbf{x}} \Theta \hat{C}_2 \text{ is Hurwitz} \}, \tag{16}$$

which corresponds to the set of controllers Θ stabilizing the augmented plant $(A, B_2^{\mathbf{x}}, C_2)$. Since there is a bijective mapping between \mathbb{A}_o and \mathbb{A}_1 , the optimization of the cost $\gamma(\mathring{\mathcal{K}})$ over $\mathring{\mathcal{K}} \in \mathbb{A}_o$ can be equivalently transformed into an optimization over $\Theta \in \mathbb{A}_1$. However, the dependence of the cost on $\Theta \in \mathbb{A}_1$ is not simple due to the fact that the closed-loop system contains unstable dynamics Λ , and the cost is defined for the stable part of the closed-loop system.

It turns out that the unstable dynamics can be isolated using a state coordinate transformation specified by the unique solution \hat{Y} to the Sylvester equation

$$\Lambda \hat{Y} - \hat{Y}(\hat{A} + \hat{B}_2^{\mathbf{x}} \Theta \hat{C}_2) = \Gamma \hat{C}_2. \tag{17}$$

The stable part of the closed-loop transfer function, $\mathfrak{F}_s(s)$, can then be parametrized by $(\Theta, \hat{Y}) \in \mathbb{A}_2$ where

$$\mathbb{A}_2 := \{ (\Theta, \hat{Y}) : \Theta \in \mathbb{A}_1, (17) \text{ holds} \}. \tag{18}$$

The reparametrization of the feasible controllers \mathbb{A}_o in terms of \mathbb{A}_2 thus reduces Problem 2 to a constrained optimization of the H_2 norm $\|\mathfrak{F}_s\|_2$ over $(\Theta, \hat{Y}) \in \mathbb{A}_2$. The problem is still difficult due to the constraint (17).

To further reduce the problem to a tractable *unconstrained* H_2 optimization, we introduce a slack variable \hat{V} as

$$\hat{V} = \hat{Y}\hat{B}_2\Psi + (I - \hat{Y}\hat{X})\Gamma,\tag{19}$$

so that the Sylvester equation (17) is written as

$$\Lambda \hat{Y} = \hat{Y}\hat{A} + \hat{V}\hat{C}_2. \tag{20}$$

This is recognized as the dual of the regulator equation

$$\hat{X}\Lambda = \hat{A}\hat{X} + \hat{B}_2\hat{U},\tag{21}$$

which is equivalent to the first condition in (9). Note that the design freedom in Γ can be equivalently captured by \hat{V} through (19) when $I - \hat{Y}\hat{X}$ is nonsingular. That is, there exists a bijective mapping between \mathbb{A}_3 and \mathbb{A}_4 , where

$$A_3 := \{(\Theta, \hat{Y}) \in A_2 : \det(I - \hat{Y}\hat{X}) \neq 0\},$$
 (22)

$$\mathbb{A}_4 := \{ (\Psi, \hat{Y}, \hat{V}) : \det(I - \hat{Y}\hat{X}) \neq 0, (20), \\ \operatorname{col}(\Psi, (I - \hat{Y}\hat{X})^{-1}(\hat{V} - \hat{Y}\hat{B}_2\Psi)) \in \mathbb{A}_1 \}.$$
 (23)

We will show that \mathbb{A}_3 is nonempty and the closure of \mathbb{A}_3 coincides with the closure of \mathbb{A}_2 when (A,B_2) is stabilizable. Therefore, under the stabilizability assumption on (A,B_2) , Problem 2 reduces to the H_2 norm optimization over $(\Psi,\hat{Y},\hat{V})\in\mathbb{A}_4$. At this point, the variables Ψ and (\hat{Y},\hat{V}) are not subject to an algebraic constraint, making the problem more tractable, unlike the case for \mathbb{A}_3 in which Θ and \hat{Y} are constrained by (17).

An additional step is necessary for further simplification of the conditions defining the set \mathbb{A}_4 , especially the stability requirement dictated by \mathbb{A}_1 . We will seek a reparametrization of Ψ so that the stability constraint in \mathbb{A}_4 can be expressed as the stability of the closed-loop system for a simple auxiliary plant and a controller Φ , where the new parameter Φ replaces Ψ . We first note that (\hat{Y}, \hat{V}) satisfies (20) if and only if

$$\hat{Y} = [Y \ \tilde{Y}], \quad \hat{V} = [\Lambda \tilde{Y} \ V], \quad (24)$$

hold for some \tilde{Y} and (Y, V) satisfying

$$\Lambda Y = YA + VC_2,\tag{25}$$

which is the dual of the first regulator equation in (9). It turns out that if we define the auxiliary controller as

$$\mathring{\Phi} = \left(\begin{array}{c|c} A_{\phi} & B_{\phi} \\ \hline C_{\phi} & D_{\phi} \end{array}\right), \quad S := (I - YX)^{-1}, \tag{26}$$

$$A_{\phi} := A_{\theta} + B_{\theta} C_2 X S \tilde{Y}, \qquad B_{\phi} := B_{\theta}, C_{\phi} := C_{\theta 1} + (D_{\theta 1} C_2 X - U) S \tilde{Y}, \quad D_{\phi} := D_{\theta 1},$$
(27)

then the design freedoms of (\hat{Y}, \hat{V}) and Ψ are captured by (Y, V, \tilde{Y}) and Φ , respectively, and the feasible controllers will be reparametrized by the bijective mapping $\mathbb{A}_4 \leftrightarrow \mathbb{A}_5$, where

$$A_5 := \{ (\Phi, Y, V, \tilde{Y}) : \det(T) \neq 0, \ T := I - XY,$$
(25), Φ stabilizes $C_2(sT - A + X\Lambda Y)^{-1}B_2 \}.$ (28)

This parametrization reduces Problem 2 to a standard H_2 optimal control problem over $\mathring{\Phi}$ when (Y, V, \tilde{Y}) is fixed so that $\det(T) \neq 0$ and (25) hold.

B. Reduction to Constrained H₂ Optimal Control

This section describes the first major step of our approach outlined in the previous section, i.e., reparametrization of the admissible controllers $\mathbb{A}_1 \leftrightarrow \mathbb{A}_2$. We will isolate the transient dynamics (i.e., stable modes) and decompose the closed-loop transfer function as in (4) so that the cost function in (5) is properly characterized. This is done by the following lemma.

Lemma 2: Consider the plant (1) and target pattern (Π, Λ) . Suppose Assumptions 1 and 2 hold. Let a controller \mathring{K} be

given by (10) with a Θ stabilizing (A, B_2^x, C_2) . Then $\mathring{\kappa} \in \mathbb{A}_o$ holds, and the cost function $\gamma(\mathring{\kappa})$ in (6) is given by

$$\gamma(\mathring{\kappa}) = \|\mathfrak{F}_s\|_2^2, \quad \mathfrak{F}_s(s) := \mathbf{C}(sI - \mathbf{A})^{-1}\mathbf{B} + \mathbf{D}, \quad (29)$$

where A is Hurwitz,

$$\mathbf{A} := \hat{A} + \hat{B}_2^{\mathbf{x}} \Theta \hat{C}_2, \quad \mathbf{C} := \hat{C}_1 + \hat{D}_1^{\mathbf{x}} \Theta \hat{C}_2 - Z \hat{Y},$$

$$\mathbf{B} := \hat{B}_1 + \hat{B}_2^{\mathbf{x}} \Theta \hat{D}_2, \quad \mathbf{D} := \hat{D}_1^{\mathbf{x}} \Theta \hat{D}_2,$$
(30)

and \hat{Y} is the unique solution to the Sylvester equation (17). Moreover, given the zero initial state and impulse input $w(t) = w_0 \delta(t)$, the closed-loop trajectory satisfies (11) with

$$\rho_o := W w_o, \quad W := \hat{Y} \mathbf{B} + \Gamma \hat{D}_2. \tag{31}$$

Proof. We designate $q(t) \in \mathbb{R}^{n_q}$ as the state vector of Θ with the state space realization in (14). Defining the coordinate

$$r := \begin{bmatrix} \chi \\ q \end{bmatrix}, \quad \chi := x - X\xi,$$
 (32)

the closed-loop system is given by

$$\begin{bmatrix} \dot{\xi} \\ \dot{r} \end{bmatrix} = \begin{bmatrix} \Lambda & \Gamma \hat{C}_2 \\ 0 & \mathbf{A} \end{bmatrix} \begin{bmatrix} \xi \\ r \end{bmatrix} + \begin{bmatrix} \Gamma \hat{D}_2 \\ \mathbf{B} \end{bmatrix} w, \tag{33}$$

where **A** is Hurwitz since Θ stabilizes $(A, B_2^{\mathbf{x}}, C_2)$. Hence, when the impulsive input $w(t) = w_o \delta(t)$ is applied, r captures the transient behavior while $\xi(t)$ converges to $e^{\Lambda t} \rho_o$ with ρ_o determined by w_o . Since $\xi(t)$ is not equal to $e^{\Lambda t} \rho_o$ for all $t \geq 0$, the transient component in $\xi(t)$ further needs to be isolated for properly characterizing the cost in (5).

Using Lemma 8 of [27], one can find a transformation that decouples the target behavior from the transient behavior and makes the system block diagonal. More specifically there exists a unique solution \hat{Y} to the Sylvester equation (17) since the spectra of Λ and \mathbf{A} are disjoint. Using \hat{Y} for the coordinate transformation, the closed-loop system in (33) is block diagonalized as

$$\dot{\rho} = \Lambda \rho + Ww, \quad \rho := \xi + \hat{Y}r,
\dot{r} = \mathbf{A}r + \mathbf{B}w,$$
(34)

with the performance output z given by

$$z = z_s + z_a$$
, $z_s := \mathbf{C}r + \mathbf{D}w$, $z_a := Z\rho$.

Hence the closed-loop transfer function $\mathfrak{F}(s)$ from w to z can be decomposed as in (4) with the stable part $\mathfrak{F}_s(s)$ given by (29). Finally, consider the response to the impulsive disturbance $w(t) = w_o \delta(t)$. Since \mathbf{A} is stable and Λ is antistable, r(t) is the transient variable that converges to zero, and $\rho(t) = e^{\Lambda t} \rho_o$ is the steady state (or persistent) variable. Then (11) follows from the definitions of the state variables.

For the controller (10), the closed-loop system is given by (33), which clearly has the Λ -eigenspace spanned by the right eigenvectors $\operatorname{col}(I,0)$ for the state $\operatorname{col}(\xi,r)$. The corresponding left eigenvectors are $\operatorname{row}(I,\hat{Y})$, where the eigenvalue-eigenvector equation is exactly given by the Sylvester equation (17). In the original state space coordinates $\mathbf{x} := \operatorname{col}(x,q,\xi)$, denote the closed-loop system with w=0 by $\dot{\mathbf{x}} = \mathbf{A}_{c\ell}\mathbf{x}$. Then its right and left eigenvectors are given by

$$\begin{aligned} \mathbf{A}_{c\ell} \mathbf{X}_{c\ell} &= \mathbf{X}_{c\ell} \boldsymbol{\Lambda}, & \mathbf{X}_{c\ell} := \operatorname{col}(\hat{X}, I), & \operatorname{row}(Y, \tilde{Y}) := \hat{Y}, \\ \mathbf{Y}_{c\ell} \mathbf{A}_{c\ell} &= \boldsymbol{\Lambda} \mathbf{Y}_{c\ell}, & \mathbf{Y}_{c\ell} := \operatorname{row}(\hat{Y}, I - YX), \end{aligned}$$

where the eigenvectors are normalized so that $Y_{c\ell}X_{c\ell} = I$. It follows from the standard system theory that the steady state response is given by $x(t) \to X_{c\ell} e^{\Lambda t} \rho_o$ with $\rho_o := Y_{c\ell} x(0)$.

A special case of this is the impulse response in Lemma 2 where the initial state $\mathbf{x}(0)$ is set from w_o so that ρ_o is given by (31). The eigenstructure analysis enabled isolation of the transient part $z_s(t)$ from the performance output z(t) so that the stable part of the closed-loop transfer function, $\mathfrak{F}_s(s)$, is explicitly characterized. The key for this isolation is the solution \hat{Y} to the Sylvester equation (17), which defines the coordinate transformation to separate transient and steady state dynamics. Problem 2 is thus equivalently reformulated in Lemma 2 as the minimization of the H_2 norm $\|\mathfrak{F}_s\|_2$ in (29) over $(\Theta, \hat{Y}) \in \mathbb{A}_2$, where \mathbb{A}_2 is defined in (18).

C. Reduction to Unconstrained H_2 Optimal Control

The constrained H_2 optimization over \mathbb{A}_2 is difficult due to the coupling of \hat{Y} and Θ through (17). For tractable reparametrizations of the admissible controllers, let us proceed to the next step in Section III-A, i.e., $\bar{\mathbb{A}}_2 = \bar{\mathbb{A}}_3$ under stabilizability of (A, B_2) , which is formally stated as follows.

Lemma 3: Consider Lemma 2 and the sets \mathbb{A}_2 and \mathbb{A}_3 defined in (18) and (22), respectively. The set \mathbb{A}_3 is nonempty if and only if (A, B_2) is stabilizable. Moreover, if \mathbb{A}_3 is nonempty, then the closures of \mathbb{A}_2 and \mathbb{A}_3 coincide.

Proof. See Appendix B.

Based on Lemma 3, under stabilizability of (A, B_2) , the optimal control that minimizes $\|\mathfrak{F}_s\|_2$ in (29) over $(\Theta, \hat{Y}) \in \mathbb{A}_2$ is obtained by minimizing the same cost function over $(\Theta, \hat{Y}) \in \mathbb{A}_3$. This is because, due to $\bar{\mathbb{A}}_2 = \bar{\mathbb{A}}_3$, any optimal control in \mathbb{A}_2 can be approached by a sequence of controllers within \mathbb{A}_3 . Thus we can restrict our search for an optimal controller within \mathbb{A}_3 . This makes the problem tractable since the regularity $\det(I - \hat{Y}\hat{X}) \neq 0$ enables a series of reparametrizations of the admissible controllers, $\mathbb{A}_3 \leftrightarrow \mathbb{A}_4 \leftrightarrow \mathbb{A}_5$ as outlined in Section III-A, leading to an unconstrained optimization. This step of the development is summarized as follows.

Lemma 4: Consider the plant (1) and target dynamics (Π, Λ) . Suppose (A, B_2) is stabilizable and Assumptions 1 and 2 hold. Then Problem 2 is equivalent to

$$\wp_* := \inf_{\mathring{\Phi} \in \mathbb{S}, Y, V} \wp(\mathring{\Phi}, Y, V), \tag{35}$$

subject to (25) and

$$\det(I - XY) \neq 0, (36)$$

where $\wp(\mathring{\Phi}, Y, V)$ is the H_2 norm squared of the closed-loop transfer function $\mathfrak{F}_s(s)$ from w to z_s for the augmented plant

$$\begin{bmatrix} T\dot{\chi}_o \\ z_s \\ y \end{bmatrix} = \begin{bmatrix} A - X\Lambda Y & B_o & B_2 \\ C_o & 0 & D_1 \\ C_2 & D_2 & 0 \end{bmatrix} \begin{bmatrix} \chi_o \\ w \\ u \end{bmatrix}, (37)$$

$$T := I - XY,$$
 $B_o := TB_1 - XVD_2,$ $S := (I - YX)^{-1},$ $C_o := C_1T - D_1UY,$ (38)

and controller $u = \Phi y$, and S is the set of controllers that internally stabilize the augmented plant. In particular,

the optimal cost values are equal to each other, $\gamma_* = \wp_*$. Moreover, given a feasible solution $(\mathring{\Phi}, Y, V)$ of (35) with $\wp_o := \wp(\mathring{\Phi}, Y, V)$, an admissible controller $\mathring{\kappa}$ given by (10) achieves the cost value $\gamma(\mathring{\kappa}) = \wp_o$, where $\mathring{\Theta}$ in (10) is specified by (14) with

$$\mathring{\Phi} = \left(\begin{array}{c|c} A_{\phi} & B_{\phi} \\ \hline C_{\phi} & D_{\phi} \end{array} \right), \tag{39}$$

$$A_{\theta} := A_{\phi} - B_{\phi}C_{2}XS\tilde{Y}, \qquad B_{\theta} := B_{\phi},$$

$$C_{\theta 1} := C_{\phi} - (D_{\phi}C_{2}X - U)S\tilde{Y}, \qquad D_{\theta 1} := D_{\phi},$$

$$C_{\theta 2} := S(\Lambda\tilde{Y} - \tilde{Y}A_{\theta} - YB_{2}C_{\theta 1}),$$

$$D_{\theta 2} := S(V - \tilde{Y}B_{\theta} - YB_{2}D_{\theta 1}),$$
(40)

with an arbitrary matrix \hat{Y} .

Proof. We first show that, given an admissible controller $\mathring{K} \in \mathbb{A}_o$, there exist a controller $\mathring{\Phi} \in \mathbb{S}$ and parameters (Y,V) such that the constraints in (25) and (36) are satisfied, and the difference in the cost value $|\wp(\mathring{\Phi},Y,V)-\gamma(\mathring{K})|$ is arbitrarily small. Fix $\mathring{K} \in \mathbb{A}_o$ as in (10) with a $\mathring{\Theta}$ in (14). From Lemma 2, there exists a solution \mathring{Y} to the Sylvester equation (17), and the cost value $\gamma(\mathring{K})$ is equal to the H_2 norm squared of $\mathfrak{F}_s(s)$ in (29). Partition Θ and \mathring{Y} to define (Ψ,Γ) and (Y,\mathring{Y}) by (15) and (24), where $Y \in \mathbb{R}^{r \times n}$. We assume, without loss of generality, that $\det(\mathring{T}) \neq 0$ for $\mathring{T} := I - \mathring{X}\mathring{Y}$, or equivalently, (36) holds. If the determinant is zero, one can redefine \mathring{K} by slightly perturbing Θ so that the determinant becomes nonzero, while keeping \mathring{K} admissible and the cost value $\gamma(\mathring{K})$ arbitrarily close to the original value. This perturbation is possible under the stabilizability of (A,B_2) due to Lemma 3.

Introducing a slack variable V, the Sylvester equation (17) is equivalently written as (25) and

$$\Gamma = (I - \hat{Y}\hat{X})^{-1}(\hat{V} - \hat{Y}\hat{B}_2\Psi), \quad \hat{V} := [\Lambda \tilde{Y} \quad V]. \tag{41}$$

The regulator equation (9) and its dual in (25) can be written

$$\hat{A}\hat{X} + \hat{B}_2\hat{U} = \hat{X}\Lambda,$$

$$\hat{Y}\hat{A} + \hat{V}\hat{C}_2 = \Lambda\hat{Y}.$$
(42)

Using (41) and (42), one can verify that the state space matrices for $\mathfrak{F}_s(s)$ in (30) are given by

$$\mathbf{A} = \hat{T}^{-1} \hat{\mathbf{A}} \hat{T}, \qquad \hat{\mathbf{A}} = \hat{A} + \hat{B}_{2} (\Psi \hat{C}_{2} - \hat{U} \hat{Y}) \hat{T}^{-1},
\mathbf{B} = \hat{T}^{-1} \hat{\mathbf{B}}, \qquad \hat{\mathbf{B}} = \hat{T} \hat{B}_{1} + (\hat{B}_{2} \Psi - \hat{X} \hat{V}) \hat{D}_{2},
\mathbf{C} = \hat{\mathbf{C}} \hat{T}, \qquad \hat{\mathbf{C}} = \hat{C}_{1} + \hat{D}_{1} (\Psi \hat{C}_{2} - \hat{U} \hat{Y}) \hat{T}^{-1},
\mathbf{D} = \hat{\mathbf{D}}, \qquad \hat{\mathbf{D}} = \hat{D}_{1} \Psi \hat{D}_{2}.$$
(43)

Now, the realization of $\mathfrak{F}_s(s)$ given by

$$\dot{r}_a = \hat{\mathbf{A}}r_a + \hat{\mathbf{B}}w, \qquad r_a := \hat{T}r = \operatorname{col}(T\chi_o, q),
z_s = \hat{\mathbf{C}}r_a + \hat{\mathbf{D}}w, \qquad \chi_o := \chi - XS\tilde{Y}q,$$
(44)

can be recognized as the closed-loop system of the augmented plant (37) and controller $\mathring{\Phi}$ in (39) specified by solving (40) for $(A_{\phi}, B_{\phi}, C_{\phi}, D_{\phi})$, where the state of $\mathring{\Phi}$ is q. Therefore, the closed-loop transfer function from w to z_s coincides with $\mathfrak{F}_s(s)$, and we conclude that $\wp(\mathring{\Phi}, Y, V) = \gamma(\mathring{K})$.

To show the converse, let a feasible (Φ, Y, V) satisfying the constraints of (35) be given, i.e., $\Phi \in \mathbb{S}$ with state space realization (39) internally stabilizes the augmented plant (37), and (Y, V) satisfies (25) and (36). Choose an arbitrary matrix

 \tilde{Y} and define $\mathring{\Theta}$ by (14) and (40), \hat{Y} by (24), and \hat{V} by (41). Then one can verify that condition (17) is satisfied by noting that (17) is equivalent to (25) and (41). Let the state space matrices for $\mathfrak{F}_s(s)$ be defined by (30). Then the closed-loop system of the augmented plant (37) and controller $\mathring{\Phi}$ (which is independent of \tilde{Y}) is given by (44) with state space matrices $(\hat{\mathbf{A}}, \hat{\mathbf{B}}, \hat{\mathbf{C}}, \hat{\mathbf{D}})$ in (43) (which apparently depends on \tilde{Y} but in fact \tilde{Y} cancels out to make it independent). This system is related to $(\mathbf{A}, \mathbf{B}, \mathbf{C}, \mathbf{D})$ in (30) by similarity transformation (43). Thus we conclude that $\wp(\mathring{\Phi}, Y, V) = \gamma(\mathring{\kappa})$.

The original problem with $(\Theta, \hat{Y}) \in \mathbb{A}_3$ in Lemma 2 is now reduced to that with $(\Phi,Y,V,\tilde{Y})\in\mathbb{A}_5$ in Lemma 4. There exists a bijective mapping between A_3 and A_5 as explained in Section III-A. The transfer function $\mathfrak{F}_s(s)$ in Lemma 2, depending on $(\Theta, \hat{Y}) \in \mathbb{A}_3$, coincides with the closed-loop transfer function from w to z_s in Lemma 4, depending on $(\Phi, Y, V, Y) \in \mathbb{A}_5$, provided (Θ, Y) and (Φ, Y, V, Y) are related by the bijective mapping. A benefit of this reparametrization is that Θ and \hat{Y} are constrained by (17) but Φ and (Y, V, Y) are independent of each other. Also, Lemma 4 shows that the freedom in \tilde{Y} can be ignored in the optimization since it does not affect the cost. With (Y, V)fixed, the minimization of $\wp(\Phi, Y, V)$ in (35) over $\Phi \in \mathbb{S}$ is a standard H_2 problem that can readily be solved. However, the optimization over the additional parameters (Y, V) still makes the problem challenging. The next section will address this issue and present the main result.

IV. AUTONOMOUS PATTERN GENERATION

A. Optimal Control for Pattern Generation

We will first solve Problem 2 without additional assumptions on the plant. The approach is to extend the linearizing change of variables in [34], [35] to deal with the additional parameters (Y, V) that are constrained by the dual regulator equation (25) and affect the cost in (35). The result is a tractable characterization of feasible controllers as follows.

Theorem 1: Consider the plant (1) and target pattern (Π, Λ) . Suppose (A, B_2) is stabilizable and Assumptions 1 and 2 hold. Let $\gamma_o \in \mathbb{R}$ be given and consider Problem 2. There exists a controller $\mathring{\kappa} \in \mathbb{A}_o$ such that the cost in (5) satisfies $\gamma(\mathring{\kappa}) < \gamma_o$ if and only if there exist parameters (P, Q, Y, V, M, G, H, L) and \mho such that $tr(\mho) < \gamma_o$,

$$\left[\begin{array}{cc} \mathbf{M} + \mathbf{M}^{\mathsf{T}} & \mathbf{H}^{\mathsf{T}} \\ \mathbf{H} & -I \end{array}\right] < 0, \quad \left[\begin{array}{cc} \mathbf{P} & \mathbf{G} \\ \mathbf{G}^{\mathsf{T}} & \mho \end{array}\right] > 0, \quad \mathbf{L} = 0, \ (45)$$

and the dual regulator equation (25) hold, where

$$\begin{bmatrix} \mathbf{M} & \mathbf{G} \\ \mathbf{H} & \mathbf{L} \end{bmatrix} := \begin{bmatrix} AQ + B_2H & AT + B_2E & TB_1 + ND_2 \\ M & PA + GC_2 & PB_1 + GD_2 \\ \hline C_1Q + D_1H & C_1T + D_1E & D_1LD_2 \end{bmatrix}$$
$$\mathbf{P} := \begin{bmatrix} Q & T \\ T^{\mathsf{T}} & P \end{bmatrix}, \quad T := I - XY, \quad \begin{array}{c} N := B_2L - XV, \\ E := LC_2 - UY. \end{array}$$

In this case, one such controller \mathring{K} is given by (10) with Θ specified by (14) and (40) with

$$\begin{split} A_{\phi} &= A + B_2 K + B_{\phi} C_2 T^{-1} + R^{-1} J, \\ B_{\phi} &= (T^{\mathsf{T}} R)^{-1} G - R^{-1} \hat{P} N, \\ C_{\phi} &= E T^{-1} - K, \\ D_{\phi} &= L, \end{split} \tag{46}$$

where \tilde{Y} in (40) is an arbitrary matrix and

$$\begin{split} J &:= \bar{\mathcal{P}} A_K + A_K^{\mathsf{T}} \bar{\mathcal{P}} + C_K^{\mathsf{T}} C_K + C_\phi^{\mathsf{T}} (K + B_2^{\mathsf{T}} \bar{\mathcal{P}} + D_1^{\mathsf{T}} C_1), \\ A_K &:= A + B_2 K, \quad C_K := C_1 + D_1 K, \\ \hat{P} &:= (T^{\mathsf{T}})^{-1} P T^{-1}, \quad R := \hat{P} - \bar{\mathcal{P}}, \quad \bar{\mathcal{P}} := Q^{-1}. \end{split}$$

Proof. See Appendix C.

For a given γ_o , the design condition given by (45), (25), and $\operatorname{tr}(\mho) < \gamma_o$ is nonconservative, and is feasible for sufficiently large γ_o , provided the stated supposition is satisfied. The condition becomes more difficult to satisfy as γ_o gets smaller, and is infeasible when γ_o is smaller than the optimal value γ_* defined in (6). Thus, Problem 2 is reduced to the minimization of $\operatorname{tr}(\mho)$ over (P,Q,Y,V,M,G,H,L) and \mho subject to (45) and (25). This is a convex optimization problem involving LMIs, and can readily be solved numerically. The optimal controller is then calculated from (46). The change of variables used in the proof of Theorem 1 is applicable not only for this H_2 control synthesis but also for other general multiobjective control problems [34] extended for autonomous pattern generation with H_∞ and various system gain performance measures.

Next, we build on Theorem 1 and derive a characterization of the optimal controller in terms of Riccati equations with the following standard assumptions [41] on the plant:

Assumption 3:

- i) (A, B_1) is stabilizable and (C_1, A) is detectable;
- ii) (A, B_2) is stabilizable and (C_2, A) is detectable;
- iii) $D_1^{\mathsf{T}}[C_1 \ D_1] = [0 \ I].$
- iv) $D_2[B_1^{\mathsf{T}} D_2^{\mathsf{T}}] = [0 \ I].$

The value of Theorem 1 is that the design process applies to a general plant with no assumptions, and it shows the proper change of variables applicable to many other cost functions than the H_2 norm, demonstrating a broader impact of our design theory. In contrast, the next result (Theorem 2) will provide an analytical insight into the optimal control architecture when the plant satisfies Assumption 3. As a design tool, Theorems 1 and 2 provide alternative methods, where the latter may be slightly preferred if the plant satisfies the assumption since commercially available software for the H_2 optimal control can be used.

We now present the solution to the standard optimal control problem for autonomous pattern generation.

Theorem 2: Consider Problem 2 for the plant (1) and target pattern (Π, Λ) . Suppose Assumptions 1, 2 and 3 hold. Let \mathfrak{P} and \mathfrak{Q} be the stabilizing solutions of the Riccati equations and define the corresponding gains:

$$\begin{array}{ll} \mathcal{P}A + A^{\mathsf{T}}\mathcal{P} - \mathcal{P}B_{2}B_{2}^{\mathsf{T}}\mathcal{P} + C_{1}^{\mathsf{T}}C_{1} = 0, & \mathcal{K} := -B_{2}^{\mathsf{T}}\mathcal{P}, \\ A\mathcal{Q} + \mathcal{Q}A^{\mathsf{T}} - \mathcal{Q}C_{2}^{\mathsf{T}}C_{2}\mathcal{Q} + B_{1}B_{1}^{\mathsf{T}} = 0, & \mathcal{F} := -\mathcal{Q}C_{2}^{\mathsf{T}}. \end{array}$$
 (47)

Let (Y, V) be a solution of

$$\varrho_* := \min_{(Y,V)} \varrho(Y,V), \quad \text{subject to} \quad YA + VC_2 = \Lambda Y,$$

where, with B_o , C_o , and T defined in (38),

$$\varrho(Y,V) := tr(\mathfrak{P}B_oB_o^{\mathsf{T}} + \mathfrak{Q}K_o^{\mathsf{T}}K_o), \quad K_o := \mathfrak{K}T + UY, = tr(\mathfrak{Q}C_o^{\mathsf{T}}C_o + \mathfrak{P}F_oF_o^{\mathsf{T}}), \quad F_o := XV + T\mathfrak{F}.$$

Then the minimum cost γ_* of Problem 2 is equal to ϱ_* , and an optimal controller that yields γ_* is given by

$$\dot{\hat{x}} = A\hat{x} + B_2 u + \mathcal{F}(C_2 \hat{x} - y),
\dot{\xi} = \Lambda \xi + (Y\mathcal{F} - V)(C_2 \hat{x} - y),
u = (U - \mathcal{K}X)\xi + \mathcal{K}\hat{x}.$$
(48)

Moreover, the trajectory of the closed-loop system, with arbitrary initial states, in response to the impulse input $w(t) = w_o \delta(t)$, converges as in (11) with

$$\rho_o := (YB_1 + VD_2)w_o + Y(x(0) - \hat{x}(0)) + \xi(0).$$

Proof. See Appendix D.

The result in Theorem 2 resembles the solution to the standard H_2 optimal control problem, including a combination of the optimal state feedback controller, the LQR with gain \mathcal{K} for (A,B_2,C_1,D_1) , and the optimal observer, the Kalman filter with gain \mathcal{F} for (A,B_1,C_2,D_2) . However, there are additional terms due to the complexity of the problem, requiring a static minimization of the cost $\varrho(Y,V)$ over (Y,V). The cost is expressed in the two alternative forms that are dual to each other. In either expression, the cost is a convex quadratic function of (Y,V) and can be minimized, subject to the linear constraint of the dual regulator equation, by standard numerical methods. In the trivial case where (X,U)=(0,0), the controller (48) reduces to the standard H_2 optimal control.

The pattern generation property of the controller (48) is rather easy to see. The closed-loop system is given by

$$\begin{bmatrix} \dot{\hat{x}} \\ \dot{\xi} \\ \dot{e} \end{bmatrix} = \begin{bmatrix} A + B_2 \mathcal{K} & B_2 (U - \mathcal{K}X) & -\mathcal{F}C_2 \\ 0 & \Lambda & (V - Y\mathcal{F})C_2 \\ 0 & 0 & A + \mathcal{F}C_2 \end{bmatrix} \begin{bmatrix} \hat{x} \\ \xi \\ e \end{bmatrix},$$

where $e:=x-\hat{x}$, assuming no input w=0. It is easy to verify that the closed-loop system has eigenvalues Λ with right eigenvector $\operatorname{col}(X,I,0)$ and left eigenvector $\operatorname{row}(0,I,Y)$. The other closed-loop eigenvalues are those of $A+B_2\mathcal{K}$ and $A+\mathcal{F}C_2$, which are Hurwitz. Thus the steady state trajectory is given by $x=\hat{x}=X\xi$ and $\xi=e^{\Lambda t}\rho_o$ with ρ_o specified by the initial state or the impulse input.

Theorem 2 revealed the fundamental feedback architecture of the optimal controller as shown in Fig. 1. The plant dynamics are copied in the blue blocks to give the standard Kalman filter plus LQR, while the red blocks embed a pattern generator (Λ dynamics). The control architecture has the same linear fractional structure as the Youla parametrization of all stabilizing controllers [36], where the central controller is the LQG controller, and the free parameter Q is set to

$$Q(s) = (U - \mathcal{K}X)(sI - \Lambda)^{-1}(Y\mathcal{F} - V),$$

which is the pattern generator $(sI - \Lambda)^{-1}$ interfaced through the feedforward gains (X, U) and feedback gains (Y, V) that are constrained by the primal and dual regulator equations:

$$AX + B_2U = X\Lambda,$$

$$YA + VC_2 = \Lambda Y.$$

In the steady state, the pattern generator creates $\xi = e^{\Lambda t} \rho_o$ without feedback since $y = C_2 \hat{x}$, and the control input $u = U \xi$ drives the plant since $\hat{x} = X \xi$. Any nonzero errors, $y - C_2 \hat{x} \neq 0$ and/or $\hat{x} - X \xi \neq 0$, would add corrective components in u to yield convergence back to the steady state.

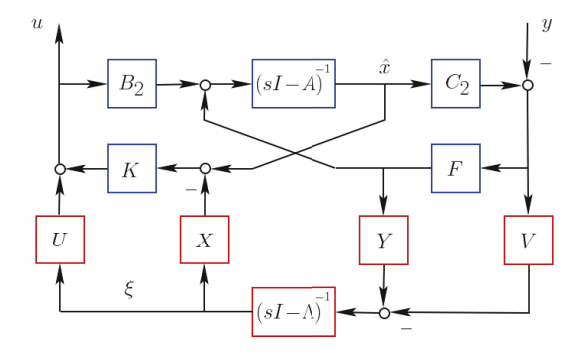


Fig. 1. The architecture of the optimal control in (48)

B. Absence of the Separation Principle

The separation principle similar to the standard H_2 optimal control does not hold for the optimal control for autonomous pattern generation. If we replace \hat{x} by x assuming state feedback in Theorem 2, the controller (48) reduces to

$$\xi = \Lambda \xi, \quad u = U\xi + \mathcal{K}(x - X\xi).$$
 (49)

However, addition of the Kalman filter to this state feedback controller is not enough for the output feedback case in general since nonzero value of (Y, V) may reduce the H_2 cost. In fact, the state feedback in (49) is not optimal as shown below.

The closed-loop system with (49) is given by

$$\begin{bmatrix} \dot{x} \\ \dot{\xi} \\ z \end{bmatrix} = \begin{bmatrix} A + B_2 \mathcal{K} & B_2 (U - \mathcal{K} X) & B_1 \\ 0 & \Lambda & 0 \\ C_1 + D_1 \mathcal{K} & D_1 (U - \mathcal{K} X) & 0 \end{bmatrix} \begin{bmatrix} x \\ \xi \\ w \end{bmatrix},$$

which has the eigenstructure $(X_{c\ell}, \Lambda)$ with $X_{c\ell} = \operatorname{col}(X, I)$, and $A + B_2 \mathcal{K}$ is Hurwitz. Hence, the state feedback controller is admissible. It can readily be verified that the transfer function \mathfrak{F}_s from w to z is stable since the Λ modes are uncontrollable, and its H_2 norm is given by $\|\mathfrak{F}_s\|_2^2 = \operatorname{tr}(B_1^\mathsf{T}\mathcal{P}B_1)$. This cost value turns out to be non-optimal:

Corollary 1: Consider Problem 2 as in Theorem 2 except that we assume y = x, i.e., $C_2 = I$ and $D_2 = 0$. Let \mathcal{P} be the stabilizing solution of the Riccati equation and define \mathcal{K} as in (47). Then the minimum cost γ_* of Problem 2 is given by

$$\gamma_* = tr(B_1^{\mathsf{T}} \mathcal{P}_{\mathbf{x}} B_1), \quad \mathcal{P}_{\mathbf{x}} := \mathcal{P} - \mathcal{P} X (X^{\mathsf{T}} \mathcal{P} X)^{-1} X^{\mathsf{T}} \mathcal{P},$$

and an optimal state feedback that yields γ_* is given by

$$\begin{split} \dot{\eta} &= \Lambda \eta + Y B_2 u - V x, & V := \Lambda Y - Y A, \\ u &= (U - \mathcal{K} X)(Y x - \eta) + \mathcal{K} x, & Y := (X^\mathsf{T} \mathcal{P} X)^{-1} X^\mathsf{T} \mathcal{P}, \end{split}$$

provided $X^{\mathsf{T}}\mathcal{P}X$ is invertible. Moreover, with the zero initial state, the trajectory of the closed-loop system in response to $w(t) = w_o \delta(t)$ converges as in (11) with $\rho_o := YB_1w_o$.

The optimal state feedback is equivalent (with a different realization) to the controller in [37], where its optimality was proven within the class of controllers of the form (10) with static Θ . The result here proves its optimality among all dynamic admissible controllers. Corollary 1 also gives an explicit formula for the optimal choice of (Y, V), which is valid when $X^{\mathsf{T}} \mathcal{P} X$ is invertible. The nonzero choice of (Y, V) reduces the cost to a value less than $\mathrm{tr}(B_1^{\mathsf{T}} \mathcal{P} B_1)$, which is the cost for the controller (49). The reduction is achieved

by the feedback to the internal model dynamics of η so that the phase and amplitude of the steady state $\eta=e^{\Lambda t}\rho_o$ is adjusted appropriately for the given impulse disturbance w. Indeed, assuming full information (i.e. not only x but also w are available for the controller), the optimal state feedback in Corollary 1 can be equivalently implemented as

$$\dot{\xi} = \Lambda \xi + Y B_1 w, \quad u = U \xi + \mathcal{K}(x - X \xi),$$

which is derived by defining $\xi := Yx - \eta$. A comparison with (49) indicates a clear advantage of the optimal control with the additional term YB_1w . Thus, the sensory feedback to the pattern generator through (Y, V) is essential.

Finally, if the separation principle holds, then the optimal controller in Theorem 2 should be recovered by adding the Kalman filter to the optimal state feedback in Corollary 1 and replacing x with \hat{x} . However, introducing the new variable $\xi := Y\hat{x} - \eta$, the process will result in the output feedback controller of the form (48) with the specific choice of (Y, V) uniquely determined by

$$Y(A + \mathcal{F}C_2) - \Lambda Y = Y_o \mathcal{F}C_2, \quad V = (Y - Y_o)\mathcal{F},$$

where $Y_o := (X^T \mathcal{D} X)^{-1} X^T \mathcal{D}$. This choice does not minimize the cost $\varrho(Y,V)$ in general (as easily shown by numerical examples), and thus the optimal output feedback controller cannot be obtained through the separation principle.

V. DESIGN EXAMPLE: INVERTED PENDULUM ON A CART A. Plant and Target Motion Patterns

We consider an inverted pendulum on a cart as shown in Fig 2. The pendulum is a point mass atop a rigid, massless rod. The control input force u is applied to the cart, and a disturbance force d acts on the pendulum point mass, resulting in the pendulum angle θ and the cart displacement x_c with no friction. The sensor reads the cart position and contains noise v.

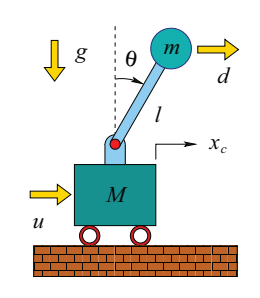


Fig. 2. The physical plant.

The equations of motion are given by

$$(M + m(1 - \cos^2 \theta)) \ddot{x}_c + f(\theta, \dot{\theta}) = u - d(1 - \cos^2 \theta),$$

$$m\ell\ddot{\theta} - mg\sin\theta + m\ddot{x}_c\cos\theta = -d\cos\theta$$
 (50)

$$f(\theta, \dot{\theta}) := mg\sin\theta\cos\theta - m\ell\dot{\theta}^2\sin\theta.$$

where M and m are the mass of the cart and pendulum respectively, ℓ is the rod length, and g is the gravity constant. The equations of motion linearized about the vertical position are assembled with performance channels to give the generalized plant (1) with

$$\begin{split} x &= \operatorname{col}(\theta, \dot{\theta}, x_c, \dot{x}_c), \\ C_1 &= \operatorname{col}(\hbar_x I, 0), \quad D_1 = \operatorname{col}(0, 1), \\ C_2 &= \operatorname{row}(0, 0, 1, 0), \quad D_2 = \operatorname{row}(0, 1), \\ \left[\begin{array}{ccc|c} A & B_1 & B_2 \end{array} \right] \\ &= \begin{bmatrix} 0 & 1 & 0 & 0 & 0 & 0 & 0 \\ \frac{(M+m)g}{M\ell} & 0 & 0 & 0 & \frac{\hbar_d}{m\ell} & 0 & \frac{-1}{M\ell} \\ 0 & 0 & 0 & 1 & 0 & 0 & 0 \\ -\frac{-mg}{M} & 0 & 0 & 0 & 0 & 0 & \frac{1}{M} \end{array} \right], \end{split}$$
 (51)

where $\hbar_x, \hbar_d \in \mathbb{R}$ are design weights, and the performance signals are defined by $w := \operatorname{col}(d/\hbar_d, v)$ and $z := \operatorname{col}(\hbar_x x, u)$.

We consider the target behavior where θ and \dot{x}_c may oscillate around a fixed value at specified frequency ω . For example, the cart may translate at a constant speed on average while the pendulum oscillates. Such behavior is captured by Λ containing an oscillatory mode and a rigid body mode:

$$\Lambda = \operatorname{diag}(\Lambda_1, \Lambda_2), \quad \Lambda_1 := \begin{bmatrix} 0 & \omega \\ -\omega & 0 \end{bmatrix}, \quad \Lambda_2 := \begin{bmatrix} 0 & 1 \\ 0 & 0 \end{bmatrix}.$$

The physical configuration of the cart-pendulum system imposes dynamic constraints that shape possible motions, which are exactly captured by the regulator equation (9). In particular, all possible motions with the Λ modes are captured by $x = Xe^{\Lambda t}\rho_o$ for some X and ρ_o , where X satisfies (9) for some U. It can readily be shown that the second entry of U can be set to zero without reducing the variety of motion patterns since the freedom can be absorbed into ρ_o . The set of all solutions (X, U) for (9), with the second entry of U being zero, is parametrized by

$$X = \begin{bmatrix} c_o & 0 & 0 & 0 \\ 0 & c_o \omega & 0 & 0 \\ -c_o \ell_o & 0 & c_1 & c_2 \\ 0 & -c_o \ell_o \omega & 0 & c_1 \end{bmatrix}, \quad U = \begin{bmatrix} c_o f_o \\ 0 \\ 0 \\ 0 \end{bmatrix}^{\mathsf{T}},$$

where c_o , c_1 , and c_2 are free parameters, and

$$\ell_o := \ell \left(1 + \frac{1}{\omega^2} \cdot \frac{g}{\ell} \right), \quad f_o := (M + m)g + M\ell\omega^2.$$

Thus, all possible motions are described by

$$\theta(t) = a_{\theta} \cos(\omega t - \phi),$$

$$x_{c}(t) = -\ell_{o}\theta(t) + v_{c}t + o_{c},$$

$$a_{\theta} := \alpha c_{o}, \quad v_{c} := c_{1}\gamma, \quad o_{c} := c_{1}\beta + c_{2}\gamma,$$

$$(52)$$

which are derived from $x=Xe^{\Lambda t}\rho_o$ with an arbitrary vector ρ_o expressed as $\rho_o:=\operatorname{col}(\alpha\cos\phi,\alpha\sin\phi,\beta,\gamma)$. We see that oscillations occur when $c_o\neq 0$, where θ and x_c must be 180^o out of phase with the amplitude ratio ℓ_o , and the cart translates at a constant average velocity when $c_1\neq 0$. In the special case where $c_o=c_1=c_2=0$, the pendulum should be stabilized vertically at the initial cart position.

The target motions (52) parametrized by (c_o, c_1, c_2) can be categorized into the six different patterns as delineated in Table I. The six motion patterns are characterized by zero/nonzero properties of the θ oscillation amplitude a_{θ} , cart average velocity v_c , and cart offset o_c , where o_c can be fixed to zero for any ρ_o only if v_c is zero. Each of c_o , c_1 , and c_2 can be restricted to 0 or 1 because patterns with any nonzero values of c_i can be captured by $c_i=1$ due to the freedom in ρ_o . Moreover, the value of c_2 does not affect the pattern and can be set to zero whenever $c_1 \neq 0$ since the offset o_c can be arbitrarily set by β . Thus we only need to consider the six cases of (c_o, c_1, c_2) in Table I.

B. Control Designs for Basic Patterns

We will first investigate the performance of the optimal linear controller (48) with the linear system (51) for the

category	c_o	c_1	c_2	amp. a_{θ}	vel. v_c	offset o_c
(i)	0	0	0	0	0	0
(ii)	0	0	1	0	0	γ
(iii)	0	1	0	0	γ	β
(iv)	1	0	0	α	0	0
(v)	1	0	1	Ω	Ω	~

TABLE I MOTION PATTERN CATEGORIES

six motion patterns in Table I. For this study, we used the following parameter values:

$$M = 2$$
 $m = 1$ $\ell = 4$, $g = 9.8$, $\omega = 2$, $\hbar_x = 1$, $\hbar_d = 200$. (53)

For each pattern, the optimal controller was designed and the closed-loop system was simulated with impulse disturbance $d(t) = \delta(t)$ while the sensor noise v and the initial plant and controller states are all set to zero.

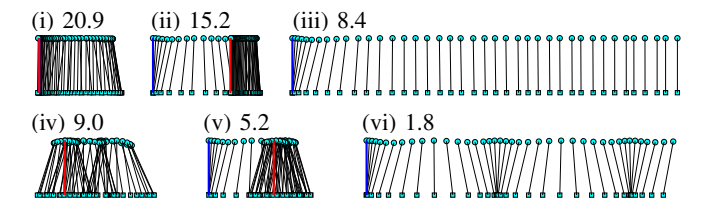


Fig. 3. Snap shots (5 frames/s) of the cart-pendulum system with the linear plant (51) and the optimal controller (48) under the impulse disturbance $d(t)=\delta(t)$ for the six patterns in Table I. The top circle and bottom square represent the pendulum point mass and the cart, respectively. Travel is to the right with the initial position indicated by the blue vertical bar. The red vertical bar indicates the cart offset o_c for the cases with $c_1=0$. The blue bar is invisible for (i) and (iv) since the red bar overlaps. The simulated time is $0 \le t \le 11$ when $c_1=0$ and $0 \le t \le 8$ otherwise. The numbers above the snapshots indicate the optimal costs in the unit of 10^6 .

The impulse responses of the cart-pendulum system are depicted in terms of the snapshots in Fig. 3. In the steady state, the pendulum converges to the vertical posture for the top row, while it oscillates for the bottom row. The (average) cart position returns to the initial position (left column), converges to an offset position o_c (middle column), or is free to travel at a constant average speed v_c (right column). The values of o_c and v_c , as well as the oscillation amplitude when allowed, are chosen by the optimal control to minimize the transient cost. Consequently, the cost is lower from left to right as we allow more freedom in the steady state pattern.

Numerical study (not shown) confirmed that different values for c_i in Table I do not affect the resulting trajectory as long as they represent the same pattern. This is due to the freedom in (Y,V), which when optimized determines the target trajectory. The implication is that for a given target pattern, there is a unique optimal target trajectory. For example, the cases with $(c_o,c_1,c_2)=(1,2,3),\ (4,5,6),\$ and (1,1,0) have different (X,U) but the optimal (Y,V) is adjusted to yield the same optimal trajectory $x=Xe^{\Lambda t}\rho_o$ uniquely determined by the impulse direction and the specified motion pattern.

C. Trajectory Replanning by Feedback to Pattern Generator

The optimal control in (48) is autonomous, embedding the pattern generator $\dot{\xi}=\Lambda\xi$ within the feedback loop. This is in contrast with the traditional output regulation architecture [6], [42] where the reference generator sits outside the feedback loop as an exosystem, providing a fixed reference command. The sensory feedback to the pattern generator allows for real-time modification of the reference trajectory ξ based on the measured output y. This section illustrates this capability and the unique attributes of our result in comparison with the traditional output regulation for tracking.

We consider the optimal controller in (48) with the target pattern specified by $(c_o,c_1,c_2)=(1,0,1)$, allowing for steady state oscillations around a fixed position. The parameter values are chosen as in (53) except for \hbar_x with a larger value $\hbar_x=100$ to make convergence faster. To illustrate the capability for trajectory replanning, we hit the system with two impulse disturbances, one at t=0 and another at t=11 s, as described by $d(t)=0.6\delta(t)+5\delta(t-11)$. The initial state is set to zero. From Theorem 2, the first impulse will result in convergence as in (11) with $\rho_o:=YB_1w_o$ and $w_o:=\operatorname{col}(0.6,0)$, and the second impulse will lead to another trajectory of the same pattern with different amplitude a_θ and location o_c , determined from the impulse and state at t=11 through $\rho_o:=YB_1w_o+Y(x(11)-\hat{x}(11))+\xi(11)$ and $w_o:=\operatorname{col}(5,0)$.

For comparison, we consider the controller obtained by setting (Y,V)=(0,0) in the optimal controller (48). In this case the pattern generator receives no feedback from the plant, and the controller is a classical regulator with the LQR and the Kalman filter, tracking a fixed reference signal from the exosystem (see Fig. 1). The regulator is evaluated by the closed-loop simulation under the same conditions as those for the optimal controller, except for the initial controller state $\xi(0)$. We choose to set $\xi(0)=YB_1w_o$ with $w_o:=\operatorname{col}(0.6,0)$ so that both controllers achieve the same trajectory after the first impulse and both plants are in (almost) the same state at the time of the second impulse.

The results are depicted in Figs. 4 and 5. For both controllers, the cart-pendulum converges to the same target trajectory after the first impulse, initially moving to the right and oscillating around a fixed cart offset o_c (red bar) in the steady state. The second impulse substantially perturbs the cart-pendulum to the right, and the classical regulator pushes it back to the previous target trajectory. However, the optimal controller finds a different target trajectory by detecting the second disturbance through sensory feedback, and makes the system oscillate around a new offset o_c (purple bar).

We now set $\hbar_x=3$, which reduces the penalty on the state variables when compared with the previous case $\hbar_x=100$. Figure 4 (iii) shows that the cart-pendulum moves further than (i) before settling down for the same magnitude of the disturbance since larger transient displacements are now allowed. This example illustrates that the steady state trajectory could be adjusted through the cost function if desired.

D. Nonlinear Augmentation of Pattern Generator

The optimal controller (48) can find a new trajectory (52) with different oscillation amplitude a_{θ} , phase ϕ , cart velocity

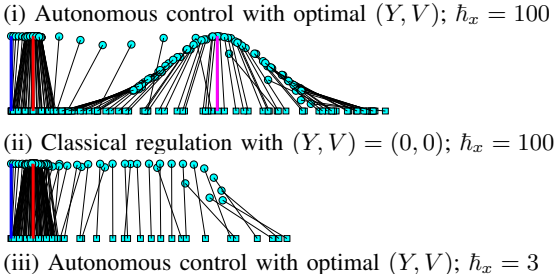




Fig. 4. Snap shots (5 frames/s) of the cart-pendulum system with the linear plant (51). The controller is given by (48) for the target pattern $(c_o, c_1, c_2) = (1, 0, 1)$, where (Y, V) is optimal for (i) and zero for (ii). Case (iii) is under the same conditions as (i) except $\hbar_x = 3$. The closed-loop system is simulated for $0 \le t \le 25$ with impulse disturbances applied twice at t = 0 and t = 11 as $d(t) = 0.6\delta(t) + 5\delta(t - 11)$.

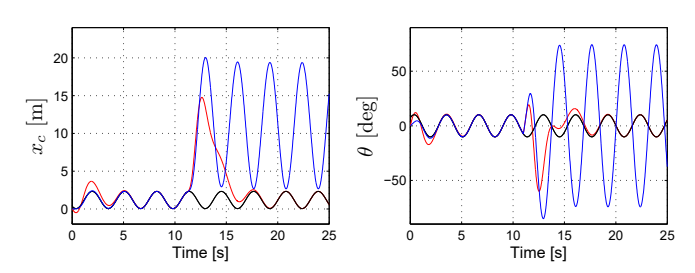


Fig. 5. The time response of the linear closed-loop system simulated under the same condition as in Fig. 4. The blue plots are for the optimal control, and the red plots are for the output regulation controller with (Y,V)=(0,0). The black plots indicate the target trajectory (11) of the optimal control in response to the first impulse disturbance.

 v_c , and offset o_c in response to a disturbance, as illustrated in the previous section. In some applications, however, it may be desired to fix some of these parameters, especially a_{θ} and/or v_c . Therefore this section suggests some heuristics to achieve convergence of these parameters to *a priori* specified values.

The idea is to augment the optimal, linear controller (48) with nonlinear components. In particular, the pattern generator dynamics Λ in the controller is replaced by the nonlinear term ${\mathfrak O}$ defined by

$$\begin{split} & \mathcal{O} = \operatorname{diag}(\mathcal{O}_1, \mathcal{O}_2), \quad \mathcal{O}_1 = \begin{bmatrix} \sigma_1 & \omega \\ -\omega & \sigma_1 \end{bmatrix}, \quad \mathcal{O}_2 = \begin{bmatrix} 0 & 1 \\ 0 & \sigma_2 \end{bmatrix}, \\ & \sigma_1 = \mu_1 (a_o^2 - \xi_1^2 - \xi_2^2), \quad \sigma_2 = \mu_2 (v_o - \xi_4), \end{split}$$

where ξ_i is the $i^{\rm th}$ entry of $\xi \in \mathbb{R}^4$, a_o is the target oscillation amplitude for ${\rm col}(\xi_1,\xi_2),\,v_o$ is the target value of the velocity variable ξ_4 , and parameters μ_1 and μ_2 weight the effects of the nonlinear components and dictate the rates of convergence (the larger, the faster). The resulting nonlinear pattern generator $\dot{\xi} = \mathcal{O}\xi$ consists of the Andronov-Hopf oscillator that has an orbitally stable limit cycle and achieves $(\xi_1,\xi_2) \to (a_o\sin(\omega t - \varphi),a_o\cos(\omega t - \varphi))$ for some constant φ when $\mu_1>0$, and the modified double integrator that achieves convergence $(\xi_3,\xi_4) \to (v_ot+\beta,v_o)$ for some constant β when $\mu_2v_o>0$. With the nonlinear augmentation of the pattern generator, the closed-loop system is expected to converge to the motion (52) as in the linear optimal control

(i) Autonomous control with linear pattern generator (optimal)



(ii) Autonomous control with nonlinear pattern generator



Fig. 6. Snap shots (5 frames/s) of the cart-pendulum system with the nonlinear plant (50). The linear optimal controller (i) is designed for $(c_o,c_1,c_2)=(1,1,0)$ using (48). The nonlinear controller (ii) is obtained as a modification of the optimal controller by replacing Λ in (48) with the nonlinear dynamics of 0 as in (54) with $\mu_1=100,\ \mu_2=0,\ a_o=0.132,$ and $v_o=0$. The closed-loop system is simulated for $0\le t\le 20$ with impulse disturbances applied twice at t=0 and t=7 as $d(t)=0.6\delta(t)-0.4\delta(t-7)$.

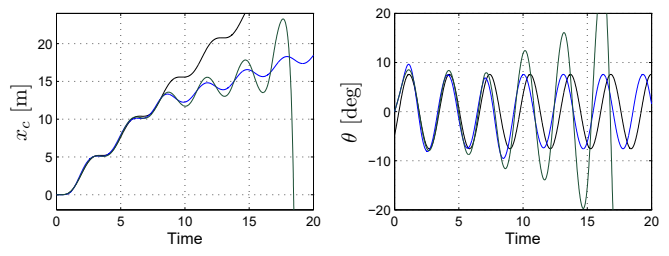


Fig. 7. The time response of the nonlinear closed-loop system simulated under the same condition as in Fig. 6. The green plots are for the linear optimal controller (i), and the blue plots are for the modified controller with the nonlinear pattern generator (ii). The black plots indicate the target trajectory of the linear optimal control in response to the first impulse disturbance.

case, with the additional property that the amplitude and velocity are fixed to $a_{\theta} = c_o a_o$ and $v_c = c_1 v_o$.

We illustrate the effectiveness of the nonlinear augmentation by design examples for the case $(c_0, c_1, c_2) = (1, 1, 0)$. The nonlinear dynamics in (50) are used for simulating the plant. Two controllers are designed: one is the linear optimal control in (48) and the other is its nonlinear augmentation as in (54). The plant and design parameters are the same as those in the previous section, i.e., (53) with modification $h_x = 100$. The closed-loop system is simulated with the zero initial state under two impulse disturbances in d with intensities +0.6 at t=0 and -0.4 at t=7, where the positive/negative signs indicate that the force is directed right/left. For the nonlinear control with (54), the velocity regulation is inactive ($\mu_2 = 0$), and the amplitude regulation is active ($\mu_1 = 100$), with the parameter a_o set so that the amplitudes of oscillations after the first impulse match those that would result if the linear optimal control were applied, i.e., $a_o = \sqrt{\rho_{o1}^2 + \rho_{o2}^2}$ with $\rho_o := Y B_1 w_o \text{ and } w_o = \text{col}(0.6, 0).$

The results are shown in Figs. 6 and 7. While the linear optimal controller is guaranteed to achieve convergence for the linear plant, it fails for the nonlinear plant; the pendulum falls toward the end of the simulation. With the nonlinear augmentation, the controller achieves convergence as intended. The oscillation amplitudes of x_c and θ (blue) converge to values close to those prescribed by a_o (black), which is clearly visible for θ . The average cart velocity \dot{x}_c converges to a constant value that depends on the disturbance as seen in the blue x_c plot that has a constant average slope after each impulse. It should be noted that the cart velocity is adjusted in response to the second disturbance as intended, while the

classical output regulation would have made the trajectory follow the black plots in Fig. 7. We also note that the phase of the oscillations (see θ plot) is not aligned with the black reference trajectory but determined by the disturbance. One may see the importance of this type of reference adaptation in some applications, observing how we recover the walking gait after tripping over a cat.

In traditional designs, a linear controller is guaranteed, by the Hartman-Grobman theorem, to stabilize an equilibrium point of a nonlinear system if it stabilizes the linearized system. In contrast, the eigenstructure assignment developed in this paper intentionally yields a controller that does not stabilize the linearized plant but makes some closed-loop eigenvalues coincide with those of Λ . As a result, the equilibrium is not hyperbolic when Λ has eigenvalues on the imaginary axis, and the solutions in the neighborhood of the equilibrium can be qualitatively different between the linear and nonlinear closed-loop systems. This is why the divergent response in Fig. 7 for the linear control is not surprising. On the other hand, the nonlinear augmentation of the pattern generator was found effective for making the target behavior structurally stable in this example, as long as the oscillation amplitude of θ remains relatively small (roughly 20°).

VI. CONCLUSION

We have developed an optimal control theory for autonomous pattern generation. The pattern describes persistent steady-state signals that are constant, growing, and/or oscillatory with fixed relative amplitudes, phases, and frequencies, while the absolute magnitude and temporal timing of the actual trajectory are part of the variables to be optimized. The controller achieves convergence to a prescribed pattern while minimizing the H_2 performance measure, i.e., the L_2 norm of the transient portion of the impulse response. The result also applies, with slight modifications, to multiobjective optimal control problems with not only H_2 but also other performance measures, exploiting the change of variables introduced in Theorem 1. Such extensions will allow for application to a wider range of problems.

The H_2 optimal controller, given in Theorem 2, is shown to embed a pattern generator within the feedback loop as an additional component to the standard Kalman filter and the LQR, possessing the same linear fractional structure as the Youla parametrization. The feedback/feedforward gains to/from the pattern generator are solutions to the regulator equation and its dual, revealing a fundamental symmetry. The autonomous control architecture, which allows for the pattern generator to receive feedback from the plant, enables modification of the target trajectory in response to disturbances. The separation principle holds in the sense that the Kalman gain and LQR gain are obtained independently, but does not hold in the sense that the optimal output feedback is not the optimal state feedback with the Kalman filter.

The stabilizability assumption on (A, B_2) is crucial for our development. If it is violated, singularity of I - XY makes a fundamental change in the optimal control problem and the main theorems become invalid. Such violation occurs in the

traditional (non-autonomous) output regulation problem where the plant dynamics are augmented with an unstable exosystem. For autonomous pattern generation, however, the stabilizability assumption would be naturally satisfied in many applications.

APPENDIX A PROOF OF LEMMA 1

The necessary and sufficient condition for \mathbb{A} to be nonempty essentially follows from Theorem 3 in [27] with a slight modification to include the nonzero D_p term in (9). Fix an admissible controller and let $X_{c\ell}$ in (3) be partitioned as $col(X, X_{\kappa})$. From Lemma 3 of [27] and its proof, an observer can be added to the controller without affecting the control input such that the new closed-loop system satisfies (3) with $X_{c\ell} = \operatorname{col}(X, X_{\kappa}^{\text{new}})$ where $X_{\kappa}^{\text{new}} := \operatorname{col}(X_{\kappa}, X)$ is full column rank. Then, from the same proof, there exists a nonsingular transformation of the controller coordinates such that the transformed augmented system satisfies (3) with $X_{c\ell} = \operatorname{col}(X, I, 0)$. Based on Theorem 3 in [27], every controller yielding $X_{c\ell}$ of this structure is necessarily captured by the formula in (10) for some Θ stabilizing the augmented plant $(A, B_2^{\mathbf{x}}, C_2)$. Finally, the cost value has been preserved during the process since neither a coordinate transformation nor the addition of an observer not connected to the control input changes the closed-loop dynamical mapping from w to z. Finally, the convergence property in (11) follows directly from the eigenstructure.

APPENDIX B PROOF OF LEMMA 3

Suppose (A,B_2) is stabilizable. Let Ψ be such that $\hat{A}+\hat{B}_2\Psi\hat{C}_2$ is Hurwitz and set $\Theta:=\operatorname{col}(\Psi,\Gamma)$ with $\Gamma=0$. Then the unique solution \hat{Y} to (17) in this case is given by $\hat{Y}=0$ since $\Gamma=0$. Hence $\det(I-\hat{X}\hat{Y})\neq 0$ and we conclude $(\Theta,\hat{Y})\in\mathbb{A}_3$. Thus stabilizability of (A,B_2) implies that \mathbb{A}_3 is nonempty.

To show the converse, suppose (A, B_2) is not stabilizable. Fix $(\Theta, \hat{Y}) \in \mathbb{A}_2$. There exists a pair of eigenvalue and left eigenvector (λ, ℓ) such that

$$\ell^* \hat{A} = \lambda \ell^*, \quad \ell^* \hat{B}_2 = 0, \quad \ell \neq 0, \quad \Re(\lambda) \ge 0.$$

Multiplying ℓ^* from left of the regulator equation (21),

$$\lambda(\ell^*\hat{X}) = (\ell^*\hat{X})\Lambda.$$

Multiplying $\ell^* \hat{X}$ from left of the Sylvester equation (17) and using the above equation,

$$\ell^*(I - \hat{X}\hat{Y})(\lambda I - \mathbf{A}) = 0.$$

Since $\Re(\lambda) \geq 0$ and \mathbf{A} is Hurwitz, $\lambda I - \mathbf{A}$ is nonsingular. Thus we have $\ell^*(I - \hat{X}\hat{Y}) = 0$, which implies $(\Theta, \hat{Y}) \notin \mathbb{A}_3$. Therefore, \mathbb{A}_3 is empty.

Finally, we show that $\bar{\mathbb{A}}_2 = \bar{\mathbb{A}}_3$ when \mathbb{A}_3 is nonempty, where $\bar{\mathbb{A}}_i$ is the closure of \mathbb{A}_i for i=2,3. For $(\Theta,\hat{Y})\in\mathbb{A}_2$, the Sylvester equation (17) uniquely determines \hat{Y} from Θ since Λ satisfies Assumption 1. Hence, $\bar{\mathbb{A}}_2 \neq \bar{\mathbb{A}}_3$ occurs only when there is a pair $(\Theta_o,\hat{Y}_o)\in\mathbb{A}_2\setminus\mathbb{A}_3$ such that every small perturbation of Θ_o to Θ and the corresponding \hat{Y} maintain $(\Theta,\hat{Y})\in\mathbb{A}_2\setminus\mathbb{A}_3$. The previous paragraph has shown that such

a pair (Θ_o, \hat{Y}_o) exists and in fact every $(\Theta, \hat{Y}) \in \mathbb{A}_2$ is such a pair, provided (A, B_2) is not stabilizable. Below, we show that such a pair does not exist when (A, B_2) is stabilizable.

Let \mathbb{A}_1 in (16) be decomposed as $\mathbb{A}_1 = \mathbb{F}_o \cup \mathbb{F}_1$ such that $\det(I - \hat{X}\hat{Y})$ is zero and nonzero for \mathbb{F}_o and \mathbb{F}_1 , respectively, where \hat{Y} is uniquely determined by (17) for $\Theta \in \mathbb{A}_1$. Suppose \mathbb{F}_o is nonempty and has an interior. We will show that $\det(I - \hat{X}\hat{Y}) = 0$ for all $\Theta \in \mathbb{A}_1$, and thus \mathbb{F}_1 is empty. This allows us to conclude that \mathbb{F}_o has no interior when \mathbb{A}_3 is nonempty and therefore $\mathbb{A}_2 = \mathbb{A}_3$.

Let the Sylvester equation (17) be written as

$$M(\theta)y = v(\theta),$$

where $\theta \in \mathbb{R}^a$ and $y \in \mathbb{R}^b$ are vectors consisting of the entries of Θ and \hat{Y} , respectively, and $M(\theta) \in \mathbb{R}^{b \times b}$ and $v(\theta) \in \mathbb{R}^b$ are affine functions of θ . Let $\mathbb{F}_v \subset \mathbb{R}^a$ be the set of vectors θ corresponding to matrices $\Theta \in \mathbb{A}_1$. Then $M(\theta)$ is square invertible for all $\theta \in \mathbb{F}_v$ since the spectra of Λ and \mathbf{A} are disjoint. For each $\theta \in \mathbb{F}_v$, we can solve the above equation for y, and then rearrange the entries of y to obtain \hat{Y} as follows:

$$y = M(\theta)^{-1}v(\theta) \implies \hat{Y} = N(\theta)/d(\theta),$$

where $d(\theta) := \det(M(\theta))$ and $N(\theta)$ is a matrix-valued polynomial of θ . Let $p(\theta)$ be the multivariate polynomial of $\theta \in \mathbb{F}_v$ defined by

$$p(\theta) := \det(d(\theta)I - \hat{X}N(\theta)) = \det(d(\theta)(I - \hat{X}\hat{Y})).$$

Now, suppose \mathbb{F}_o is nonempty and has an interior. Then there exist $\theta_o \in \mathbb{F}_v$ and its neighborhood $\mathbb{N}(\theta_o) \subset \mathbb{R}^a$ such that $\theta_o \in \mathbb{N}(\theta_o) \subset \mathbb{F}_v$ and $p(\theta) = 0$ for all $\theta \in \mathbb{N}(\theta_o)$. Since the multivariate polynomial $p(\theta)$ vanishes on an open set, $p(\theta)$ must be identically zero. Hence $\det(I - \hat{X}\hat{Y}) = 0$ for all $\Theta \in \mathbb{A}_1$ and thus \mathbb{F}_1 is empty.

APPENDIX C PROOF OF THEOREM 1

From Lemma 4, Problem 2 reduces to the optimization in (35). In particular, there exists a controller $\mathring{\kappa} \in \mathbb{A}_o$ such that $\gamma(\mathring{\kappa}) < \gamma_o$ if and only if there exist $\mathring{\Phi} \in \mathbb{S}$ and (Y,V) such that (25) and (36) hold, and the H_2 norm squared of $\mathfrak{F}_s(s) = \hat{\mathbf{C}}(sI - \hat{\mathbf{A}})^{-1}\hat{\mathbf{B}} + \hat{\mathbf{D}}$ is less than γ_o , where $\mathfrak{F}_s(s)$ is the transfer function of the closed-loop system with the augmented plant (37) and $u = \mathring{\Phi}y$. By a standard linear system theory, $\|\mathfrak{F}_s\|_2^2 < \gamma_o$ holds if and only if there exist symmetric matrices $\hat{\mathbf{P}}$ and \mathcal{V} such that $\mathrm{tr}(\mathcal{V}) < \gamma_o$, $\hat{\mathbf{D}} = 0$, and

$$\hat{\mathbf{P}}\hat{\mathbf{A}} + \hat{\mathbf{A}}^{\mathsf{T}}\hat{\mathbf{P}} + \hat{\mathbf{C}}^{\mathsf{T}}\hat{\mathbf{C}} < 0, \quad \hat{\mathbf{P}} > 0, \quad \hat{\mathbf{B}}^{\mathsf{T}}\hat{\mathbf{P}}\hat{\mathbf{B}} < \mho,$$

which are equivalent, via the Schur complement, to

$$\begin{bmatrix} \hat{\mathbf{P}}\hat{\mathbf{A}} + \hat{\mathbf{A}}^{\mathsf{T}}\hat{\mathbf{P}} & \hat{\mathbf{C}}^{\mathsf{T}} \\ \hat{\mathbf{C}} & -I \end{bmatrix} < 0, \quad \begin{bmatrix} \hat{\mathbf{P}} & \hat{\mathbf{P}}\hat{\mathbf{B}} \\ \hat{\mathbf{B}}^{\mathsf{T}}\hat{\mathbf{P}} & \mho \end{bmatrix} > 0. (55)$$

Since the order of the controller $\mathring{\Phi}$ can be chosen equal to the plant order due to Lemma 4, one can choose the controller state coordinates so that $\hat{\mathbf{P}}$ has the following special structure [34], [35]:

$$\hat{\mathbf{P}} = \begin{bmatrix} \hat{P} & R \\ R & R \end{bmatrix}, \quad Q := (\hat{P} - R)^{-1}.$$

Consider bijective mapping $\Phi \leftrightarrow (M, G, H, L)$ specified by

$$=\begin{bmatrix}M&G\\H&L\end{bmatrix}$$

$$=\begin{bmatrix}T^{\mathsf{T}}R&T^{\mathsf{T}}\hat{P}B_{2}\\0&I\end{bmatrix}\begin{bmatrix}A_{\phi}&B_{\phi}\\C_{\phi}&D_{\phi}\end{bmatrix}\begin{bmatrix}-Q&0\\C_{2}T^{-1}Q&I\end{bmatrix}$$

$$+\begin{bmatrix}T^{\mathsf{T}}\hat{P}(A-B_{2}UYT^{-1})Q&-T^{\mathsf{T}}\hat{P}XV\\-UYT^{-1}Q&0\end{bmatrix}.$$

Using the regulator equation (9) and its dual (25), we have

$$\begin{bmatrix} \mathbf{T} & 0 \\ 0 & I \end{bmatrix}^{\mathsf{T}} \begin{bmatrix} \hat{\mathbf{P}}\hat{\mathbf{A}} & \hat{\mathbf{P}}\hat{\mathbf{B}} \\ \hat{\mathbf{C}} & \hat{\mathbf{D}} \end{bmatrix} \begin{bmatrix} \mathbf{T} & 0 \\ 0 & I \end{bmatrix} = \begin{bmatrix} \mathbf{M} & \mathbf{G} \\ \mathbf{H} & \mathbf{L} \end{bmatrix},$$
$$\mathbf{T}^{\mathsf{T}}\hat{\mathbf{P}}\mathbf{T} = \mathbf{P}, \quad \mathbf{T} := \begin{bmatrix} Q & T \\ -Q & 0 \end{bmatrix}.$$

The condition (45) now follows from the congruence transformation of (55) using **T**. Thus, given a controller $\mathring{\Phi}$ such that $\|\mathfrak{F}_s\|_2 < \gamma_o$, there exist (P,Q,Y,V,M,G,H,L) and \mho satisfying $\mathrm{tr}(\mho) < \gamma_o$ and (45). Conversely, if such parameters exist, then the corresponding controller $\mathring{\Phi}$ can be obtained through the bijective mapping. In particular, the simple formula for $\mathring{\Phi}$ is obtained as such solution after a modification such that a new feasible M is chosen as

$$M = -(AT + B_2E)^{\mathsf{T}} - (C_1T + D_1E)^{\mathsf{T}}(C_1Q + D_1H), (56)$$

to make the (1,2) and (2,1) blocks of $\mathbf{M} + \mathbf{M}^{\mathsf{T}} + \mathbf{H}^{\mathsf{T}} \mathbf{H}$ equal to zero. Finally, the description of the controller \mathring{K} follows from Lemma 4.

APPENDIX D PROOF OF THEOREM 2

We will fix (Y,V) and consider the minimization of γ_o over parameters (P,Q,M,G,H,L) and \mho subject to $\operatorname{tr}(\mho)<\gamma_o$, (45), and (25). Let γ_\star be the optimal value. We will first show that $\varrho(Y,V)$ is a lower bound on γ_\star . We then show that the lower bound can actually be achieved by the controller (48).

Let γ_o be an arbitrary number larger than γ_\star . Then Theorem 1 implies that there exist (P,Q,M,G,H,L), and \mho such that $\mathrm{tr}(\mho)<\gamma_o$ and (45) hold. Note that $\mathbf{L}=0$ implies L=0 since D_1 and D_2^{T} both have full column rank. The first condition in (45) is equivalent to

$$\mathbf{M} + \mathbf{M}^{\mathsf{T}} + \mathbf{H}^{\mathsf{T}} \mathbf{H} < 0. \tag{57}$$

Partition the left-hand side into 2×2 blocks in accordance with the definition of M. Then the (1,1) and (2,2) blocks are negative definite, i.e.,

$$\begin{aligned} & \operatorname{He}(AQ + B_2 H) + C_Q^{\dagger} C_Q < 0, \\ & \operatorname{He}(PA + GC_2) + C_o^{\dagger} C_o < 0, \\ & C_Q := C_1 Q + D_1 H. \end{aligned} \tag{58}$$

Note that the first condition in (58) can be expressed as

$$\begin{split} & \operatorname{He} \big(\bar{\mathcal{P}}(A + B_2 K) \big) + (C_1 + D_1 K)^{\mathsf{T}} (C_1 + D_1 K) < 0, \\ \bar{\mathcal{P}} &:= Q^{-1}, \quad K := HQ^{-1}. \end{split}$$

From Lemma 5 in Appendix F, we have $\mathcal{P} \leq \bar{\mathcal{P}}$. Now, the second condition in (45) implies

$$\begin{bmatrix} S & SB_1 + SFD_2 \\ (SB_1 + SFD_2)^{\mathsf{T}} & \mho - B_o{}^{\mathsf{T}} \mathcal{P} B_o \end{bmatrix} > 0,$$

where we used the Schur complement and $\mathcal{P} \leq \bar{\mathcal{P}}$, and

$$S := P - T^{\mathsf{T}} \mathfrak{P} T, \quad F := S^{-1} (G + T^{\mathsf{T}} \mathfrak{P} X V).$$

The above inequality, the second condition in (58), and ${\rm tr}(\mho) < \gamma_o$ imply

$$\operatorname{tr}(B_o^{\mathsf{T}} \mathfrak{P} B_o) + \operatorname{tr}(B_1 + F D_2)^{\mathsf{T}} S(B_1 + F D_2) < \gamma_o,$$

 $S(A + F C_2) + (A + F C_2)^{\mathsf{T}} S + K_o^{\mathsf{T}} K_o < 0,$

where the last term of the above Lyapunov inequality is found by using the regulator equation (9), its dual (25), and the first Riccati equation in (47) to eliminate V, Λ , and then A, respectively. Note that S>0 by definition since $\mathbf{P}>0$ and $\bar{\mathcal{P}}\geq \mathcal{P}$, and the above Lyapunov inequality then implies that $A+FC_2$ is Hurwitz. Noting that the above inequalities define an H_2 norm bound on a linear system in terms of the observability Gramian S, the condition implies existence of an upper bound $\bar{\mathbb{Q}}>0$ on the controllability Gramian, satisfying

$$\operatorname{tr}(B_o^{\mathsf{T}} \mathcal{P} B_o) + \operatorname{tr}(K_o \bar{\mathcal{Q}} K_o^{\mathsf{T}}) < \gamma_o, \operatorname{He}((A + FC_2) \bar{\mathcal{Q}}) + (B_1 + FD_2)(B_1 + FD_2)^{\mathsf{T}} < 0.$$
 (59)

By Lemma 5, the second inequality implies $Q \leq \bar{Q}$ for (any) solution Q of the second Riccati equation in (47). Thus we have $\varrho(Y,V) < \gamma_o$. Since γ_o can be arbitrarily close to γ_\star , we conclude that $\varrho(Y,V)$ is a lower bound on γ_\star .

The controller formula is derived as follows. When Lemma 5 is applied to show $\mathcal{P} \leq \bar{\mathcal{P}}$ and $\mathcal{Q} \leq \bar{\mathcal{Q}}$ above, it suggested the best choices of the parameters that give the lower bounds: $K = \mathcal{K}$ for $\bar{\mathcal{P}} = \mathcal{P}$, and $F = \mathcal{F}$ for $\bar{\mathcal{Q}} = \mathcal{Q}$. Based on these, we set the parameters in (46) as

$$\begin{split} K &= \mathcal{K}, \quad G = S \mathcal{F} - T^{\mathsf{T}} \mathcal{P} X V, \\ Q^{-1} &= \mathcal{P}, \quad R^{-1} = T S^{-1} T^{\mathsf{T}}, \quad \hat{P} = R + \mathcal{P}. \end{split}$$

We then obtain

$$\begin{split} D_{\phi} &= 0, \\ C_{\phi} &= -UYT^{-1} - \mathcal{K}, \\ B_{\phi} &= T\mathcal{F} + XV, \\ A_{\phi} &= A + B_2\mathcal{K} + (T\mathcal{F} + XV)C_2T^{-1}, \end{split}$$

where we noted that J=0. Substituting these into (40) to find $\mathring{\Theta}$, we have

$$\begin{split} A_{\theta} &= A + B_2 \mathcal{K} + B_{\theta} C_2, & B_{\theta} &= T \mathcal{F} + X V, \\ C_{\theta 1} &= -\mathcal{K}, & D_{\theta 1} &= 0, \\ C_{\theta 2} &= D_{\theta 2} C_2, & D_{\theta 2} &= V - Y \mathcal{F}, \end{split}$$

where we chose $\tilde{Y} := Y$ to simplify the equations. An optimal controller is then found from (10) as

$$\dot{q} = Aq + B_2(U\xi - u) + B_\theta \varepsilon,
\dot{\xi} = \Lambda \xi + (V - Y\mathcal{F})\varepsilon,
u = U\xi - \mathcal{K}q, \quad \varepsilon := y - C_2(X\xi - q).$$

Defining $\hat{x} := X\xi - q$, the controller is given by (48).

Finally, we need to verify that the controller is admissible and attains the lower bound $\varrho(Y,V)$ on the optimal cost γ_* since the above process found an optimizer on the boundary of the open feasible set defined by (45). It can readily be verified that the closed-loop system can be described as

$$\begin{bmatrix} \dot{\eta} \\ \dot{h} \\ \dot{e} \\ z \end{bmatrix} = \begin{bmatrix} \Lambda & 0 & 0 & YB_1 + VD_2 \\ 0 & A + B_2 \mathcal{K} & -B_\theta C_2 & -B_\theta D_2 \\ 0 & 0 & A + \mathcal{F}C_2 & B_1 + \mathcal{F}D_2 \\ Z & C_1 + D_1 \mathcal{K} & C_o & 0 \end{bmatrix} \begin{bmatrix} \eta \\ h \\ e \\ w \end{bmatrix},$$

$$\eta := \xi + Ye, \quad e := x - \hat{x}, \quad h := \hat{x} - X\xi.$$

Thus the transfer function $\mathfrak{F}_s(s)$ from w to $z_s := z - Z\eta$ is stable, and its H_2 norm is characterized by the controllability Gramian diag (S, \mathbb{Q}) , where S is the solution to

$$(A + B_2 \mathcal{K})S + S(A + B_2 \mathcal{K})^{\mathsf{T}} + B_{\theta} B_{\theta}^{\mathsf{T}} = 0,$$

and the H_2 norm is given by

$$\|\mathfrak{F}_s\|_2^2 = \operatorname{tr}(C_1 + D_1 \mathfrak{K}) S(C_1 + D_1 \mathfrak{K})^{\mathsf{T}} + \operatorname{tr}(C_o \mathfrak{Q} C_o^{\mathsf{T}}).$$

Noting that $(C_1 + D_1 \mathcal{K}, A + B_2 \mathcal{K})$ has the observability Gramian \mathcal{P} and using duality, the first term is equal to $\operatorname{tr}(F_o{}^\mathsf{T}\mathcal{P}F_o)$ and thus we have $\|\mathfrak{F}_s\|_2^2 = \varrho(Y,V)$ as claimed. The dual formula for $\varrho(Y,V)$ can be derived similarly. Finally, the description for the steady state trajectory of the impulse response follows by noting from the closed-loop equation that e and h converge to zero and $\eta = e^{\Lambda t} \rho_o$.

APPENDIX E PROOF OF COROLLARY 1

We follow the same process as in the proof of Theorem 2 up to (59). For the state feedback case, the infimum of $\bar{\Omega}$ is given by $\bar{\Omega} = 0$, and the cost γ_o is bounded below by $\operatorname{tr}(TB_1)^{\mathsf{T}}\mathcal{P}(TB_1)$, or the trace of

$$(Y - (X^\mathsf{T} \mathcal{P} X)^{-1} X^\mathsf{T} \mathcal{P})^\mathsf{T} (X^\mathsf{T} \mathcal{P} X) (Y - (X^\mathsf{T} \mathcal{P} X)^{-1} X^\mathsf{T} \mathcal{P}) + \mathcal{P}_\mathbf{x}.$$

This lower bound can be approached by choosing

$$Y = (X^{\mathsf{T}} \mathcal{P} X)^{-1} X^{\mathsf{T}} \mathcal{P}, \quad F = -I/\varepsilon,$$

with small $\varepsilon > 0$. With a coordinate transformation, the dynamics of controller (48) can be written as

$$\dot{\eta} = \Lambda \eta + Y B_2 u - V x, \quad \eta := Y \hat{x} - \xi,
\dot{e} = (A + \mathcal{F})e - B_1 w, \quad e := \hat{x} - x.$$

With $\mathcal{F}=F=-I/\varepsilon$, the impulse response of the error e converges to zero arbitrarily fast as $\varepsilon \to 0$. In the limit, we have $\hat{x}=x$ and the optimal state feedback as stated in the corollary.

APPENDIX F TECHNICAL LEMMA

The following lemma shows that every solution of the Lyapunov inequality for a state feedback problem is bounded below by every solution of the corresponding Riccati equation.

Lemma 5: Suppose

$$\begin{split} &P(A+BK) + (A+BK)^\mathsf{T} P + (C+DK)^\mathsf{T} (C+DK) \leq 0, \\ & \mathfrak{P} A + A^\mathsf{T} \mathfrak{P} - (\mathfrak{P} B + C^\mathsf{T} D) (\mathfrak{P} B + C^\mathsf{T} D)^\mathsf{T} + C^\mathsf{T} C = 0, \\ & D^\mathsf{T} D = I, \quad A + BK \text{ is Hurwitz.} \end{split}$$

Then we have $\mathcal{P} < P$ and

$$\begin{split} & \mathcal{P}(A+B\mathcal{K}) + (A+B\mathcal{K})^{\mathsf{T}}\mathcal{P} + (C+D\mathcal{K})^{\mathsf{T}}(C+D\mathcal{K}) = 0, \\ & \mathcal{K} := -(B^{\mathsf{T}}\mathcal{P} + D^{\mathsf{T}}C). \end{split}$$

Proof. Let the left-hand side of the first inequality be denoted by W. Then the following identity holds:

$$(P-\mathcal{P})(A+BK)+(A+BK)(P-\mathcal{P})=W-(K-\mathcal{K})^{\mathsf{T}}(K-\mathcal{K}).$$

Then stability of A+BK and $W\leq 0$ imply $P\geq \mathcal{P}$. It is easy to verify that the Lyapunov equation for \mathcal{P} is equivalent to the Riccati equation.

REFERENCES

- [1] S. Strogatz, Sync. New York, NY: Hachette Books, 2003.
- [2] M. Mesbahi and M. Egerstedt, Graph Theoretic Methods in Multiagent Networks. Princeton University Press, 2010.
- [3] F. Dorfler and F. Bullo, "Synchronization in complex networks of phase oscillators: A survey," *Automatica*, vol. 50, no. 6, pp. 1539–1564, 2014.
- [4] S. Knorn, Z. Chen, and R. Middleton, "Overview: Collective control of multiagent systems," *IEEE Trans. Contr. Network Sys.*, vol. 3, no. 4, pp. 334–347, 2016.
- [5] B. Francis and W. Wonham, "The internal model principle of control theory," *Automatica*, vol. 12, no. 5, pp. 457–465, 1976.
- [6] B. Francis, "The linear multivariable regulator problem," SIAM J. Control Optim., vol. 15, no. 3, pp. 486–505, 1977.
- [7] C. Byrnes and A. Isidori, "Limit sets, zero dynamics, and internal models in the problem of nonlinear output regulation," *IEEE Trans. Auto. Contr.*, vol. 48, no. 10, pp. 1712–1723, 2003.
- [8] J. Huang and Z. Chen, "A general framework for tackling the output regulation problem," *IEEE Trans. Auto. Contr.*, vol. 49, no. 12, pp. 2203– 2218, 2004.
- [9] M. Dimitrijevic, Y. Gerasimenko, and M. Pinter, "Evidence for a spinal central pattern generator in humans," *Annals of New York Academy of Sciences*, vol. 860, no. 1, pp. 360–376, 1998.
- [10] S. Grillner, "Biological pattern generation: the cellular and computational logic of networks in motion," *Neuron*, vol. 52, no. 5, pp. 751–766, 2006.
- [11] A. Ijspeert, "Central pattern generators for locomotion control in animals and robots: A review," *Neural Networks*, vol. 21, pp. 642–653, 2008.
- [12] T. Iwasaki, J. Chen, and W. O. Friesen, "Biological clockwork underlying adaptive rhythmic movements," *Proc. Nat. Aca. Sci.*, vol. 111, no. 3, pp. 978–983, 2014.
- [13] R. Kier, J. Ames, R. Beer, and R. Harrison, "Design and implementation of multipattern generators in analog VLSI," *IEEE Trans. Neural Networks*, vol. 17, no. 4, pp. 1025–1038, 2006.
- [14] M. Lodi, A. Shilnikov, and M. Storace, "Design of synthetic central pattern generators producing desired quadruped gaits," *IEEE Trans. Circ. Syst.*, vol. 65, no. 3, pp. 1028–1039, 2018.
- [15] A. Wu and T. Iwasaki, "Design of controllers with distributed CPG architecture for adaptive oscillations," *Int. J. Robust and Nonlin. Contr.*, vol. 31, no. 2, pp. 694–714, 2021.
- [16] L. Pecora and T. Carroll, "Master stability functions for synchronized coupled systems," *Physical Review Letters*, vol. 80, no. 10, pp. 2109– 2112, 1998.
- [17] A. Pogromsky, G. Santoboni, and H. Nijmeijer, "Partial synchronization: from symmetry towards stability," *Physica D*, vol. 172, pp. 65–87, 2002.
- [18] Q. Pham and J. Slotine, "Stable concurrent synchronization in dynamic system networks," *Neural Networks*, vol. 20, pp. 62–77, 2007.
- [19] L. Scardovi and R. Sepulchre, "Synchronization in networks of identical linear systems," *Automatica*, vol. 45, pp. 2557–2562, 2009.
- [20] X. Liu and T. Iwasaki, "Design of coupled harmonic oscillators for synchronization and coordination," *IEEE Trans. Auto. Contr.*, vol. 62, pp. 3877–3889, 2017.
- [21] P. Wieland, R. Sepulchre, and F. Allgower, "An internal model principle is necessary and sufficient for linear output synchronization," *Automatica*, vol. 47, pp. 1068–1074, 2011.
- [22] L. Zhu, Z. Chen, and R. Middleton, "A general framework for robust output synchronization of heterogeneous nonlinear networked systems," *IEEE Trans. Auto. Contr.*, vol. 61, no. 8, pp. 2092–2107, 2016.
- [23] H. Kim, H. Shim, and J. Seo, "Output consensus of heterogeneous uncertain linear multi-agent systems," *IEEE Trans. Auto. Contr.*, vol. 56, no. 1, pp. 200–206, 2011.
- [24] T. Yang, A. Saberi, A. Stoorvogel, and H. Grip, "Output synchronization for heterogeneous networks of introspective right-invertible agents," *Int. J. of Robust and Nonlinear Control*, vol. 24, no. 13, pp. 1821–1844, 2014.
- [25] T. Motoyama and K. Cai, "Top-down synthesis of multiagent formation control: An eigenstructure assignment based approach," *IEEE Trans. Contr. Network Syst.*, vol. 6, no. 4, pp. 1404–1414, 2019.
- [26] S. Galeani and M. Sassano, "Modal consensus, synchronization and formation control with distributed endogenous internal models," *Automatica*, vol. 95, pp. 163–171, 2018.
- [27] A. Wu and T. Iwasaki, "Pattern formation via eigenstructure assignment: General theory and multi-agent application," *IEEE Trans. Auto. Contr.*, vol. 63, no. 7, pp. 1959–1972, 2018.
- [28] B. Moore, "On the flexibility offered by state feedback in multivariable systems beyond closed loop eigenvalue assignment," *IEEE Trans. Auto. Contr.*, vol. 21, no. 5, pp. 689–692, 1976.

- [29] M. Fahmy and J. O'Reilly, "On eigenstructure assignment in linear multivariable systems," *IEEE Trans. Auto. Contr.*, vol. 27, no. 3, pp. 690–693, 1982.
- [30] A. Andry, E. Shapiro, and J. Chung, "Eigenstructure assignment for linear systems," *IEEE Trans. Aerosp. Electron. Syst.*, vol. 19, no. 5, pp. 711–729, 1983.
- [31] K. Sobel and E. Shapiro, "Eigenstructure assignment for design of multimode flight control systems," *IEEE Contr. Sys. Mag.*, vol. 5, no. 2, pp. 9–15, 1985.
- [32] M. Rastgaar, M. Ahmadian, and S. Southward, "A review on eigenstructure assignment methods and orthogonal eigenstructure control of structural vibrations," *Shock and Vibration*, vol. 16, 2009.
- [33] A. Saberi, A. Stoorvogel, P. Sannuti, and G. Shi, "On optimal output regulation for linear system," *Int. J. Contr.*, vol. 76, no. 4, pp. 319–333, 2003
- [34] C. Scherer, P. Gahinet, and M. Chilali, "Multiobjective output-feedback control via LMI optimization," *IEEE Trans. Auto. Contr.*, vol. 42, no. 7, pp. 896–911, 1997.
- [35] I. Masubuchi1, A. Ohara, and N. Suda, "LMI-based controller synthesis: A unified formulation and solution," *Int. J. Robust Nonlinear Contr.*, vol. 8, no. 2, pp. 669–686, 1998.
- [36] D. Youla, H. Jabr, and J. Bongiorno, "Modern Wiener-Hopf design of optimal controllers – Part II: The multivariable case," *IEEE Trans. Auto. Contr.*, vol. 21, pp. 319–338, 1976.
- [37] T. Ludeke and T. Iwasaki, "Linear quadratic regulator for autonomous oscillation," *Proc. American Contr. Conf.*, pp. 4891–4896, 2019.
- [38] K. Zhou, J. Doyle, and K. Glover, Robust and Optimal Control. Prentice Hall, 1996.
- [39] M. Rotea, "The generalized H₂ control problem," Automatica, vol. 29, no. 2, pp. 373–386, 1993.
- [40] R. Olfati-Saber and R. Murray, "Consensus problems in networks of agents with switching topology and time-delays," *IEEE. Trans. Auto. Contr.*, vol. 49, no. 9, pp. 1520–1533, 2004.
- [41] J. Doyle, K. Glover, P. Khargonekar, and B. Francis, "State-space solutions to standard H_2 and H_{∞} control problems," *IEEE Trans. Auto. Contr.*, vol. 34, no. 8, pp. 831–847, 1989.
- [42] A. Astolfi, "Tracking and regulation in linear systems," Encyclopedia of Systems and Control, Springer-Verlag London, 2014.



Taylor Ludeke received her B.S. degree in Applied Mathematics from the University of Virginia, and after some industrial experience, including an engineering position at the Aerospace Corporation, received her Ph.D degree in Mechanical and Aerospace Engineering from the University of California, Los Angeles in 2020. Her expertise areas include dynamical systems analysis, animal locomotion mechanisms, and optimal control theory. She is also passionate about teaching and currently works as science instructor at the St. Francis High School.



Tetsuya Iwasaki (M'90-SM'01-F'09) received his B.S. and M.S. degrees in Electrical and Electronic Engineering from the Tokyo Institute of Technology in 1987 and 1990, and his Ph.D. degree in Aeronautics and Astronautics from Purdue University in 1993. He held faculty positions at Tokyo Tech and University of Virginia before joining the UCLA.

His current research interests include dynamics and control of neuromechanics, global pattern formation via local interactions, and robust/optimal control theories and their applications to engineering

systems. He has received several awards from NSF, SICE, IEEE, and ASME. He has served as Senior/Associate Editor of several control journals.